Chapter 1
Introduction

Supersonic combustion in a scramjet engine has been investigated widely for decades [1]. With digging deeper into the supersonic combustion issues, the hot spot has been shifted gradually from quasi-steady state such as flame stabilization to unsteady state such as combustion fluctuations. Nowadays, unsteady supersonic combustion and its control strategy pose a big challenge for real scramjet engine applications.

In the supersonic combustor, chemical reaction and heat release occur in a high-speed and high-enthalpy stream, resulting in the intense combustion unsteadiness. There are many issues affecting the unsteady supersonic combustion that need to be investigated. The mechanisms of the unsteady supersonic combustion can be roughly divided into five categories based on the dominating factors, i.e., the interactions between acoustic wave and flame, flow dominating instability, ignition unsteadiness, flame flashback, and near-blowout combustion.

The combustion generally emerges in the subsonic regions generated by the flame-holder in the combustor. In the subsonic region, acoustic waves can propagate freely upstream and affect the mixing and reaction process. Once the acoustic waves couple with the heat release processes, the thermo-acoustic instabilities could be induced in the combustion.

Due to the pressure rise in the combustion region, boundary layer separation generally occurs upstream, and the shock train is also induced. Oscillations of the shock train along with the separated regions dominate the flow in the combustor and change the mixing and reaction conditions. The intrinsic unsteadiness in the flow field could become a certain cause of unsteady combustion.

Ignition is a transition process from the unreacted state to the consistently reacted state. As the beginning phase of combustion, it is vitally important to the combustion instability. The forced ignition methods are widely used in the scramjet combustor, and the influencing factors still need to be investigated. Under certain conditions, auto-ignition is significant and also affects both the ignition process and the consistently reacted state. Thus, the effects of the ignition on combustion instability deserve particular attention.

M. Sun et al., *Unsteady Supersonic Combustion*,
https://doi.org/10.1007/978-981-15-3595-6_1

During the combustion, transient flame flashback was observed under some occasions. The flow conditions rapidly change in the combustor when flame flashback emerges. It is an important sub-process of the combustion oscillation. The flame flashback is a complex unsteady combustion phenomenon coupled with deflagration–detonation transition, boundary layer separation, and thermal choking.

When the flow condition is near the blowout limits, the combustion characteristics are concerned specially and important for understanding the instability mechanism. The combustion instability is observed remarkably increasing when the flow condition approaching the blowout limits. These unsteady phenomena are frequently encountered and closely related to the combustion dynamics in supersonic combustors. They raise a great challenge in organizing the supersonic combustion.

This book describes the unsteady phenomena for understanding supersonic combustion. It is organized into five chapters. This chapter introduces the basic thoughts and important researches in the unsteady supersonic combustion. In Chaps. 2–5, the recent studies of the unsteady phenomena are described; such as the interactions between acoustic wave and flame, flow dominating instability, ignition instability, flame flashback, and near-blowout combustion.

1.1 Interactions Between Acoustic Wave and Flame

In many low-speed combustion systems, acoustic waves can be easily excited and sustained in the confined volume, and the frequency ranges of high-amplitude pressure oscillations are close to those of the natural acoustic modes in those systems. The high-amplitude pressure oscillations arise from the feedback loop between acoustic waves and unsteady heat release. It is a common assumption that acoustic waves cannot travel upstream in a supersonic flow, and any flow oscillations arising in the flame zone will simply travel downstream and exit from the engine without forming the feedback loop required to sustain combustion and flow instabilities. However, there are various subsonic flow regions in scramjets. In these subsonic flow regions, the acoustic wave can propagate towards upstream and lead to unsteady combustion ultimately. So, researches on oscillatory phenomena and mechanisms about thermoacoustic instabilities with experiment or numerical simulation play a decisive role in the development of supersonic combustion systems.

Before introducing the acoustic vibration modes of the combustion chamber, it is necessary to give a brief review and description of the related concept of the acoustic wave and acoustic oscillations.

1.1.1 Fundamentals of the Coupling Between Acoustic Wave and Combustion Process

The coupling between the acoustic wave and combustion process was discovered by Higgins in 1777. Many researches have been carried out to investigate the mechanism of the coupling between the acoustic wave and the combustion process.

Rayleigh criterion [2], as an universal explanation for the coupling between acoustic wave and combustion process, is used in many theoretical researches on thermoacoustic instabilities in combustion systems. The criterion replaces the burning process by a hypothetical heating process, and the combustion process is simplified to an interaction of heat release and acoustic field.

Rayleigh criterion gives the condition for thermoacoustic instability and is described as the following equation:

$$\iint_V p'(x,t)q'(x,t)dtdV \geq \iint_V \sum_{i=1} L_i(x,t)dtdV \tag{1.1}$$

where $p'(x,t)$ is the pressure fluctuations, $q'(x,t)$ is the heat release fluctuations, $L_i(x,t)$ is the energy loss of acoustic wave. The unsteady heat release delivered energy to acoustic filed is not necessarily to bring sustaining instability. Only when the rhythms of working fluids movements and fluctuations are in accordance with thermal processes, will the thermoacoustic oscillations be held.

The Rayleigh criterion shows the coupling between acoustic wave and heat release fluctuations. However, a variety of complex physical processes may be involved in the combustion process. Some of the interactions during the coupling between the acoustic wave and combustion process have been given in Fig. 1.1. It is important to understand the elementary processes of interaction between combustion and waves

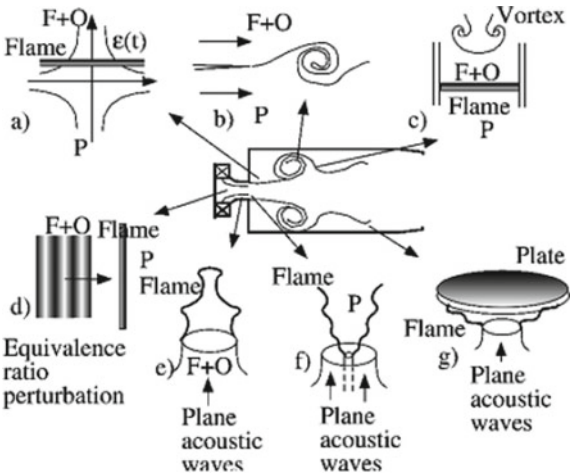

Fig. 1.1 Elementary processes: **a** unsteady strained diffusion flame, **b** unsteady strained premixed flame, **c** premixed flame/vortex interaction, **d** equivalence ratio perturbation interacting with a premixed flame, **e** acoustically modulated conical flame, **f** acoustically modulated V flame, and **g** perturbed flame interacting with a plate [3]

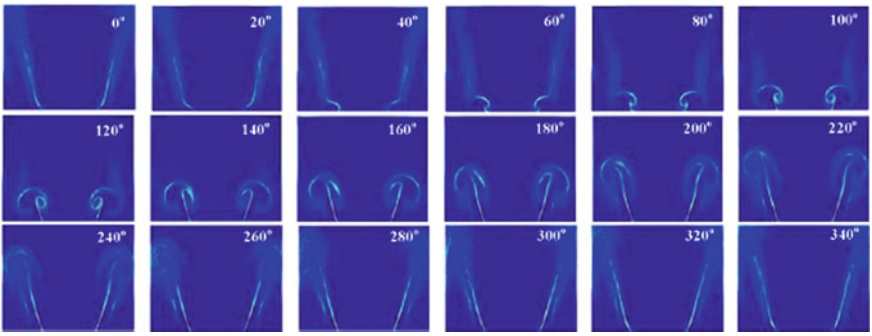

Fig. 1.2 Phase-averaged flame surface density image sequence under strong acoustic forcing [4]

or flow perturbations (acoustics, convective modes, injection inhomogeneities, etc.), which may become driving or coupling processes under unstable conditions. In this section, the influence of vortex (flow instabilities) and injection inhomogeneities will be introduced.

Experiments and theoretical analysis indicate that certain types of instabilities in lean premixed combustors may be driven by perturbations in the fuel and air ratio. This is illustrated here by assuming that pressure oscillations in the combustor interact with the fuel supply line and change the fuel flow rate. A positive pressure excursion produces a decrease in the fuel supply at a later instant. This causes a negative perturbation in the equivalence ratio, which is then convected by the flow to the flame zone. The interaction may also take place with the air supply, and this will also affect the equivalence ratio. The fluctuation of the equivalence ratio leads to a fluctuation of the heat release, and if the fluctuation of heat release is in phase with the pressure oscillation, energy may be fed into the resonant acoustic mode involved in the combustion process. Vortex structures drive various types of combustion instabilities, and the evolution of the vortex in one period can be observed in Fig. 1.2. In many premixed systems, the ignition and delayed combustion of these structures constitute the mechanism that feeds energy into the oscillation. The process involves at least two distinct mechanisms. In the first, the flame area is rapidly changing in the presence of a vortex, and the change of the flame area leads to a fluctuation of heat release. In the second, the vortex interacts with a wall, or another structure, inducing a sudden ignition of fresh material. Rollup by a vortex often controls the mixing of fresh gases into the burning regions, and this determines the unsteady rate of conversion of reactants in the flow and the amplitude of the pressure pulse resulting from the vortex burnout. The fluctuation of heat release will feed back to the combustion process, and the unsteady combustion will be intensified if these processes are in phase with the pressure fluctuation.

1.1.2 Classification of Combustion Instability Related to Acoustic Wave

Historically, the combustion instabilities are classified according to their frequency range, but between the so-called low frequency, intermediate frequency and high frequency, there is no clear borderline.

1.1.2.1 Low-Frequency Instability

The frequency of low-frequency combustion instability is usually below 200 Hz, mainly caused by the coupling of the combustion process in the combustion chamber and the flow process of the propellant feed system, and it is usually related to the ignition quality and injection speed of the propellant entering the combustion chamber. Ignition quality includes ignition delay time, flame propagation speed and flame stability characteristics. Combustion chamber, the scale of the propellant pipeline and the flow rate and mixing ratio of the propellant have a key role in the low-frequency oscillations. Coupling of the combustion process and the injector structure can also cause low-frequency instability: injector may work like a diaphragm, and produce an "Oiler"-type oscillation, causing inhomogeneous propellant injection and atomization, resulting in low-frequency instability. Some other situations can also result in the coupling between the combustion (or chamber pressure) and structure system and cause low-frequency instability. For example, the perturbation of chamber pressure makes the cooling jacket bend, causing pressure oscillations of the propellant contained in the cooling jacket. This coupling can lead to low-frequency instability.

When low-frequency combustion instability occurs, the wavelength of the gas oscillation is usually much larger than the characteristic length of the chamber or the supply system. Therefore, it can be considered that, the pressure oscillation of combustion chamber is uniformly distributed in any instantaneous, and it can be seen as the oscillations of the whole gas field in the combustion chamber; Meanwhile, the pipeline of propellant supply system or liquid collection chamber also exhibits oscillations. This instability is often a sine wave with low amplitude at the beginning, and then developed linearly into a higher amplitude.

In different types of combustion instabilities, low-frequency instability is probably the easiest one to deal with from a viewpoint of theoretical and experimental analysis or development. From the standpoint of theoretical analysis, the combustion chamber can be simulated by using a concentrated volume element, and the combustion is represented by a simple constant time delay, the resistance of propellant supply system is neglected, although the inertia and capacity of the supply system may be important in the analysis. Combustion time delay is defined as: the time required for the liquid propellant to be completely vaporized and consumed. An experiential average value can often be obtained for each propellant. The time delay usually referred to is the flight time of the component with the worst volatility from the injector surface to the impinging point. Because it is a major part of the

total time delay. Methods to eliminate low-frequency instabilities include increasing the injector pressure drop, increasing fluid inertia, as well as reducing the volume of the combustion chamber, and so on. For approaches used to change the time delay, some are successful, but some are problematic since they may degrade system performance or cause high-frequency instability though they can successfully eliminate low-frequency instability.

1.1.2.2 High-Frequency Instability

High-frequency instability is a result of combustion processes coupled with the combustor acoustic oscillations, also known as resonant combustion or acoustic instability. The oscillation frequency is usually above 1000 Hz. When high-frequency combustion instability occurs, for the measured dynamic pressure in the combustion chamber at different locations, the relationship between the oscillation frequency and the phase of each point is often consistent with the natural modes of acoustic modes of the combustion chamber. Thus, according to the acoustic characteristics of the combustion chamber, high-frequency instability can be divided into the axial (longitudinal) or horizontal (radial and tangential) mode. The above various modes of high-frequency combustion instability can be divided according to their order of resonance into the first-order vibration mode, the second-order vibration mode, etc., such as first-order radial vibration mode, second-order longitudinal vibration mode and third-order tangential vibration mode. The heat release rate varies when the flame is under different vibration mode, which can be observed from Fig. 1.3.

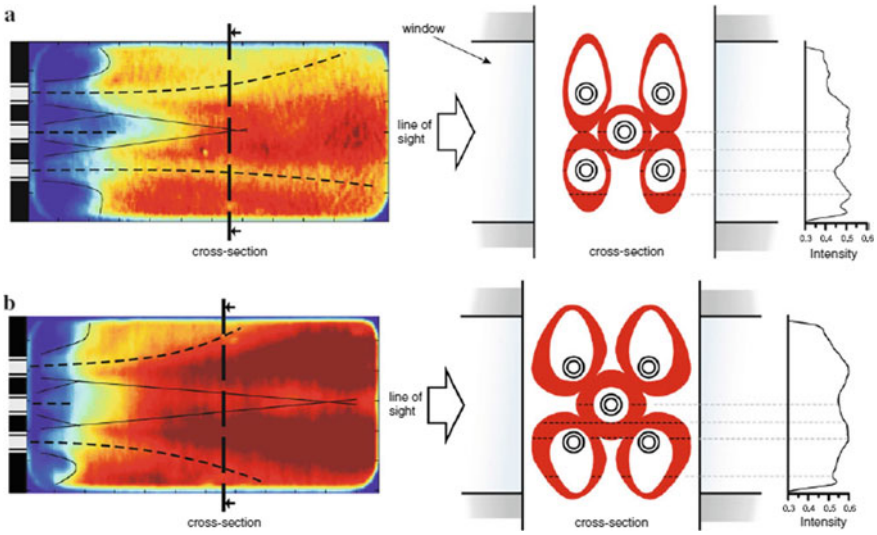

Fig. 1.3 Flame cross-sectional intensity profiles extracted from time-averaged OH* images during; **a** off-resonance, and **b** 1T mode excitation [5]

For the mechanism of high-frequency instability, current points of view include: ignition time lag, sensitive chemical time lag, physical time lag, detonation process, the changes of chemical reaction rate caused by the fluctuations of pressure or temperature, the "explosion" when the droplets are heated to beyond its critical temperature and critical pressure, and the jet flow, liquid fan or the crushing and mixing of liquid droplets.

To maintain high-frequency instability, firstly, there must be an oscillating energy to maintain the high-frequency instability of liquid rocket engine. The energy comes from the combustion of the propellant; secondly, the oscillation energy must be added at appropriate time phase related to oscillating pressure. Therefore, the methods to eliminate high-frequency instability usually have two categories: (1) change propellant spray combustion field or pressure wave characteristics, so that the energy released by the combustion fluctuations is less than the oscillation energy required to maintain oscillation, such as baffle devices; (2) change the dynamic energy loss or damping, making it greater than the energy obtained from combustion response, such as various different types of damping devices.

1.1.2.3 Intermediate-Frequency Instability

Intermediate-frequency combustion instability is the oscillation caused by the coupling between the combustion process in the combustion chamber and a portion of flow processes of the propellant supply system. The frequency range is usually 200–1000 Hz, lying between high and low-frequency oscillations.

When intermediate-frequency combustion instability occurs, it is often accompanied by a gradually increased combustion noise with a specific frequency, and its amplitude increases slowly. Besides the gas oscillations, fluctuations usually appear in the propellant supply system, the frequency and phase of gas oscillation are not consistent with the inherent acoustic modes of the combustion chamber, which is different from the high-frequency combustion instability. On the other hand, it is also different from the low-frequency combustion instability. Because its frequency is slightly higher, the wavelength of gas oscillation is close to or slightly larger than the characteristic length of the combustion chamber, so fluctuations in the combustion chamber and the supply system pipeline cannot be ignored; The pressure oscillation in combustion chamber will change spatially, and cannot be seen as a whole gas field like that in low-frequency combustion instability. Intermediate-frequency combustion instability may lead to oscillations of the propellant mixture ratio and decrease of engine performance.

1.1.3 Acoustic Induced Combustion Instabilities in Supersonic Flows

The experience with airbreathing propulsion systems and rocket engines suggests that combustion instability coupled to thermoacoustic may present an important obstacle in the development of scramjet engines. It is a common assumption that acoustic waves cannot travel upstream in a supersonic flow, any flow oscillations arising in the flame zone will simply travel downstream and exit from the engine without forming the feedback loop required to sustaining combustion and flow instabilities. In reality, with an experimental investigation, Stamp et al. [6] have found that acoustic waves can propagate upstream in various subsonic-flow regions and a scramjet combustor may be susceptible to acoustic-feedback type self-sustained combustion instabilities. Besides, the interactions between injector flows, shock waves, and boundary layers have strong unsteady characteristics and may cause instabilities in a supersonic combustor. The Acoustic-convective feedback loops in supersonic flow have been given in Fig. 1.4. Cavity flameholders increase the resonance of a sound and may introduce additional oscillation mechanisms to the combustor. The cavity-induced oscillations, on the one hand, can enhance the fuel-air mixing. On the other hand, they couple the internal and external regions, making the cavity flow fields highly complicated and even causing combustion instabilities [7].

Choi et al. [9, 10] carried out a comprehensive numerical analysis for both nonreacting and reacting flows in a scramjet engine combustor with and without a cavity. The results showed a wide variety of phenomena resulting from the interactions between the injector flows, shock waves, boundary layers, and cavity flows. Flow oscillations caused by the cavity overrode those induced by the interactions between shock waves and boundary layers, the captured high-frequency oscillations were associated with the cavity and flow unsteadiness. However, further investigations are required to achieve a better understanding of detailed fluid and flame dynamics and acoustic characteristic in a scramjet combustor.

Ma et al. [11] observed the low-frequency oscillations at 100–160 Hz for liquid JP-7 fuel and 300–350 Hz for gaseous ethylene in a dual-mode scramjet by using frequency pressure sensors. The low-frequency oscillations for liquid JP-7 can be observed in Fig. 1.5. A quasi-one-dimensional model to simulate the main features of the oscillatory flow fields in both the isolator and combustor was established, and the flow oscillations were reproduced by the numerical results. The mechanism responsible for driving flow oscillations was identified as the acoustic-convective

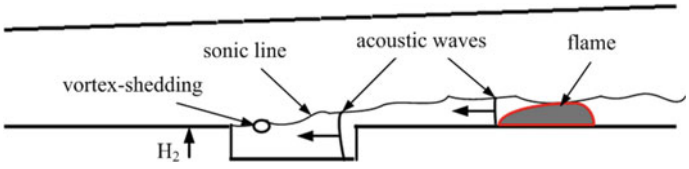

Fig. 1.4 Acoustic-convective feedback loops [8]

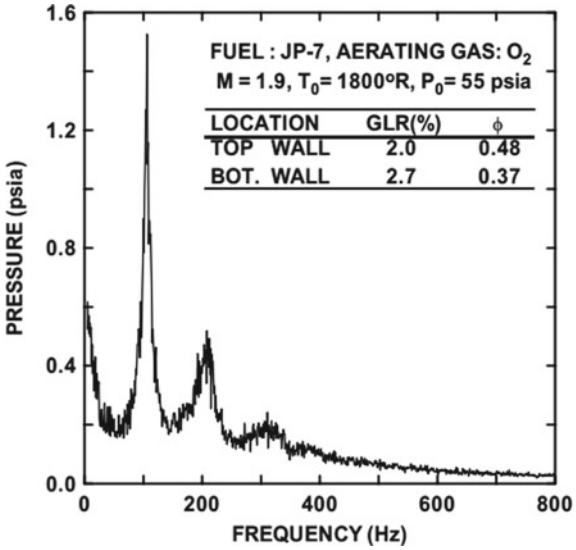

Fig. 1.5 Typical pressure power spectrum inside a scramjet combustor with liquid JP-7 fuel [11]

interactions between the fuel injector and the flame zone. Li et al. [12] carried out three-dimensional simulation of the ethylene-fueled scramjet combustor investigated by Ma et al. [11]. The results displayed the oscillations of the flame and fuel distribution.

Lin et al. [13] investigated acoustic oscillation instabilities inside an ethylene-fueled supersonic combustor with a recessed cavity flameholder. The schematic in Fig. 1.6 shows the flow-path with key combustor features identified. Under various flow conditions and flameholder geometries, the acoustic signals were recorded by high-speed pressure transducers positioned at the base and downstream of the cavity flameholder. The effects of fuel/air equivalence ratio, fueling scheme, cavity length, and simulated flight conditions on the stability characteristics of the combustor were examined systematically, and the results of the pressure oscillations for various fueling schemes and equivalence ratios can be observed in Fig. 1.7. In order

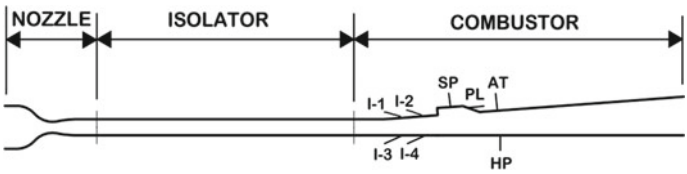

Fig. 1.6 Schematic of the combustor flowpath and key interior features (AT, Air throttle; HP, High-speed pressure transducer; I-1, Body side first row 15° gaseous injectors; I-2, Body side second row 15° gaseous injectors; I-3, Cowl side first row 15° gaseous injectors; I-4, Cowl side second row 15° gaseous injectors; PL, Pilot fuel injectors; SP, Spark plugs) [13]

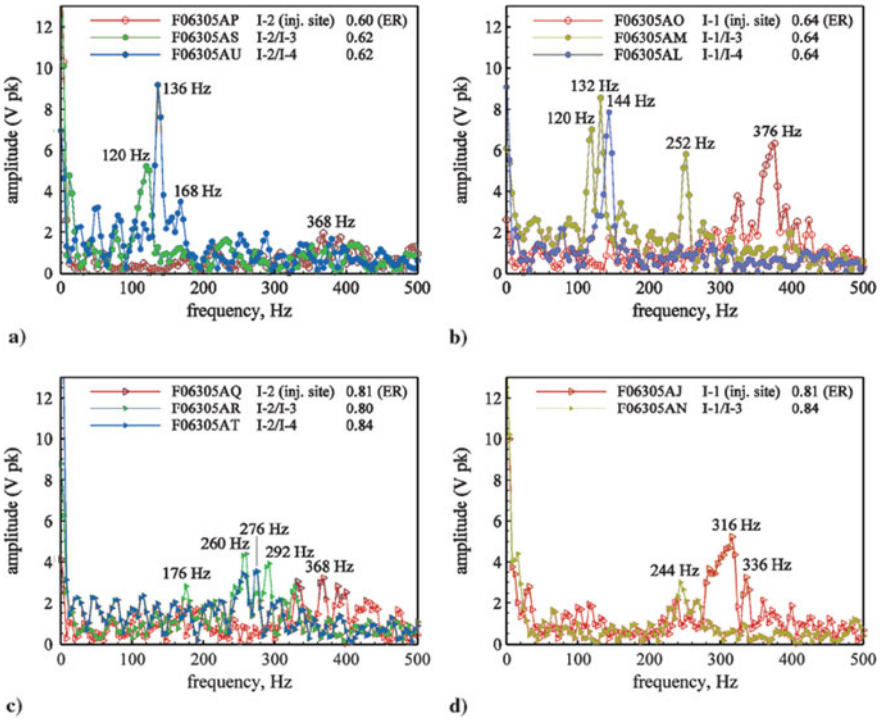

Fig. 1.7 Frequency spectra of pressure oscillations for various fueling schemes and equivalence ratios [13]

to explain these observed frequencies characteristic, three prospective mechanisms were identified in Lin's research [13].

The first and second mechanisms were concerned with the coupling between the terminal shock and flame zone. The shock-flame acoustic feedback loop was established by the upstream propagation of acoustic waves produced in the combustor and the interaction of these acoustic disturbances with the shock wave in the isolator. Then the perturbations traveled downstream as acoustic or entropy waves, enhancing the unsteady combustion in the flame zone.

The third mechanism described the interaction of acoustic waves and fluctuation happened in the region between the fuel injection and flame zone, where disturbances from the flame zone propagated upstream and caused an air mass flow-rate oscillation in the fuel injection region. For comparison, some acoustic admittance equations were used to estimate characteristic times and corresponding oscillation frequencies, and the measured oscillation frequencies agreed well with the characteristic frequencies related to each acoustic feedback loop between the shock and flame or the feedback loop between the fuel injector and flame.

As indicated by the feedback mechanisms, it is reasonable to believe that these instabilities basically occur in the ramjet mode rather than in the scramjet mode since

the large subsonic regions behind the pre-combustion shock seem necessary for the acoustic waves to readily propagate upstream.

1.1.4 Summary

As this review of the research efforts on studying the interaction between acoustic wave and combustion process, many experimental, numerical simulation and theoretical works have been done to observe and measure the characteristic of combustion oscillation. It is found that acoustic wave can propagate to upstream in the channel with a supersonic main flow. Some feedback loop of acoustic wave between combustor and isolator are proposed to predict the characteristic time and corresponding oscillation frequencies for comparison with experimental data. Thus, the differences of configuration or coupling mechanism cause disparities on spectra of frequency, which demonstrate their association with acoustic wave.

1.2 Flow Dominating Instability

The shock dominated flow is typical in supersonic combustion, and the intrinsic unsteadiness of flowfield plays a key role under some occasions. Boundary layer separation often occurs in combustor due to combustion-induced pressure rise [14]. Oscillation of shock train along with the separated regions is a certain cause of unsteady combustion.

1.2.1 Low-Frequency Unsteadiness of Shock Wave/Turbulent Boundary Layer Interaction

Shock wave/boundary-layer interactions (SWBLI) represent complex flow phenomena that are associated with a wide range of flows, including transonic airfoils, supersonic inlets, over-expanded nozzles, etc. Often the shock induces significant boundary layer separation, which leads to a highly unsteady flow field [15].

The unsteadiness of SWBLI consists of a high-frequency component and a low-frequency component [16]. Figure 1.8 depicts pressure power spectra in a Mach 5 compression ramp from five different locations taken by Erengil and Dolling [17]. The high-frequency peak of pressure fluctuations from locations 1, 4 and 5 are around the outer-scale frequency, U_∞/δ_0. The high-frequency oscillation of location 1 is determined by fluctuations from the upstream boundary layer, and the unsteadiness of the separation bubble is affected by radiation from the turbulent shear layer above. However, the pressure power spectra of stations 2 and 3 represent a dominant peak

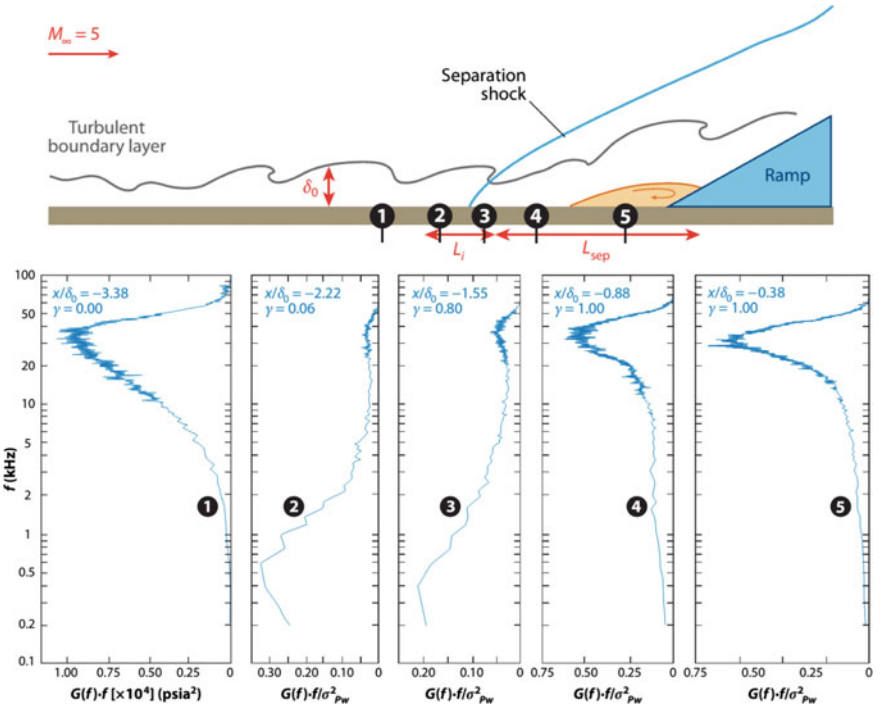

Fig. 1.8 Pressure power spectra underneath the interaction generated by a 28° compression ramp in a Mach 5 flow [23]

at a much lower frequency, which is of order 0.01 U_∞/δ_0. Such a low-frequency unsteadiness depicts the oscillation frequency of the separation shock foot. These basic trends in the power spectra of pressure fluctuations remain nearly the same for other traditional interactions, including those generated by ramps with sweep [18, 19], blunt [20] and sharp fins [21], and reflected shocks [22].

The shock foot unsteadiness in SWBLI is a typical low-frequency oscillation in supersonic flow, whose characteristics can be described as follows. The shock foot undergoes larger-scale motion and lower oscillation frequencies as the scale of separation increases. The dimensionless frequency Strouhal number however, is nearly the same [23] (Ma = 3: St = 0.09 and 0.11 [24], Ma = 2.3: St = 0.03, 0.035 and 0.04 [22]). The dimensionless frequency can be calculated as follows:

$$S_t = f L_{sep}/U_\infty \tag{1.2}$$

where f is the peak frequency of static pressure oscillation, L_{sep} is the time-averaged separated flow length, and U_∞ is the free stream velocity. Compared to the high-frequency unsteadiness, the mechanism of low-frequency oscillations remains not fully explained.

Previous researches mainly describe the unsteady flow by pressure data, which is usually not enough for mechanism study. In recent years, more and more studies try to uncover the mechanism of low-frequency unsteadiness with advanced experimental and computational methods. Humble et al. [25] carried out an experimental study to investigate the three-dimensional instantaneous structures of an incident SWTBLI at Mach 2.1. The large-scale coherent motions within the incoming boundary layer were observed using tomographic particle image velocimetry. As shown in Fig. 1.9, the instantaneous reflected shock wave pattern was found to be consistent with the streamwise-elongated low- and high-speed regions as they enter the interaction. Priebe et al. [26] characterized the low-frequency unsteadiness of a SWTBLI generated by a compression ramp at Mach 2.9. With the direct numerical simulation (DNS), the low-frequency streamwise oscillation of the shock wave was captured. The statistical relation between the low-frequency shock motion and the upstream/downstream flow was analysed. The changes in the velocity and vorticity profiles in the initial part of the interaction were found to be affected by an inherent instability in the downstream separated flow. On the other hand, the statistical relation of the shock motion and the upstream boundary layer was rather weak.

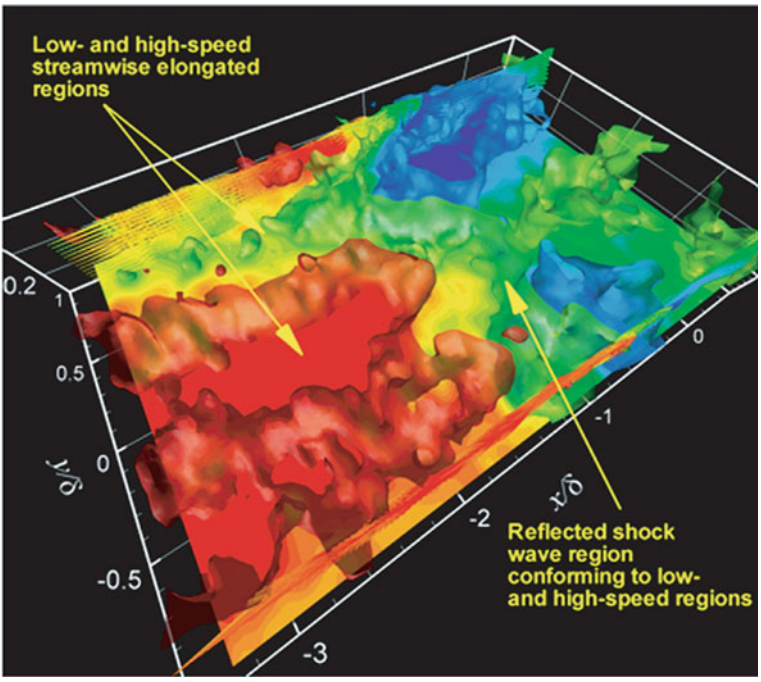

Fig. 1.9 Volumetric representations of the instantaneous flow organization of the interaction: lower region ($z/\delta = 0.1$–0.6). Iso-surfaces of streamwise velocity are shown: relatively high-speed in red ($0.9\ U_\infty$), intermediate velocity in green ($0.75\ U_\infty$), and relatively low-speed in blue ($0.55\ U_\infty$). Velocity vectors are shown flooded with instantaneous streamwise velocity [25]

Pasquariello et al. [27] analysed the low-frequency dynamics of a high Reynolds number impinging SWTBLI at Mach 3. The large-eddy simulation (LES) was performed for a very long integration time to obtain a trustworthy result for the strong separated flow. Consistent with experimental data, the simulated power spectral densities (PSD) of wall-pressure exhibited an energetic, broadband and low-frequency component associated with the separation-shock unsteadiness. Sparsity-promoting dynamic mode decompositions (SPDMD) yielded a classical low-frequency breathing mode of the separation bubble, as well as a medium-frequency shedding mode responsible for reflected and reattachment shock corrugation.

Based on numerous researches implemented all over the world, some preliminary work on modeling the low-frequency unsteadiness in SWTBLI was established. Piponniau et al. [28] developed a model to describe the properties of fluid entrainment in the mixing layer generated downstream of the separation shock. The model well estimated the low-frequency shock unsteadiness observed in various shock-induced separation cases ranging from Mach 0 to 5. It was concluded that the main source of low-frequency unsteadiness was the dynamics of the separated bubble. Due to the complexity in low-frequency unsteadiness in SWTBLI, its mechanism is still not fully explained so far. In general, it is acknowledged [23] that the downstream mechanism dominates for strongly separated flows, and a combined mechanism (both upstream and downstream) dominates for weakly separated flows.

1.2.2 Unsteadiness of Shock-Induced Separation in Non-reacting Flow

Unsteadiness of flow separation has been widely investigated in non-reacting flows, such as the inlet of the unstart process, isolator under strong backpressure and nozzle in over-expanded condition.

Studies of the unsteady shock motions in inlets mainly focused on the unstart process. Koo et al. [29] studied an inlet-isolator configuration with large eddy simulation. The unstart dynamics were fully simulated under three different inlet ramp angles (0, 6, and 8°). It was found that the separated boundary layers on both walls played key roles in the initiation of the unstart process. Simulated results indicated that the unstart shock propagation was accelerating during the unstart process, as in Fig. 1.10. However, the propagation speed of the shock train from LES was 3–4 times larger than the experiment due to the simplified models for the boundary layers. Do et al. [30] injected a transverse jet into a supersonic inlet flow to induce unstart. They concluded that thick turbulent boundary layers in asymmetric boundary conditions would prompt the formation of unstart shocks. On the other hand, the symmetric boundary conditions led to the propagation of pseudo-shocks. Zhang et al. [31] carried out an experimental study in a hypersonic inlet with side compression at a freestream Mach number of 6.0. A flow plug was placed at the duct exit to simulate the combustion induced high pressure. During the retreating process of

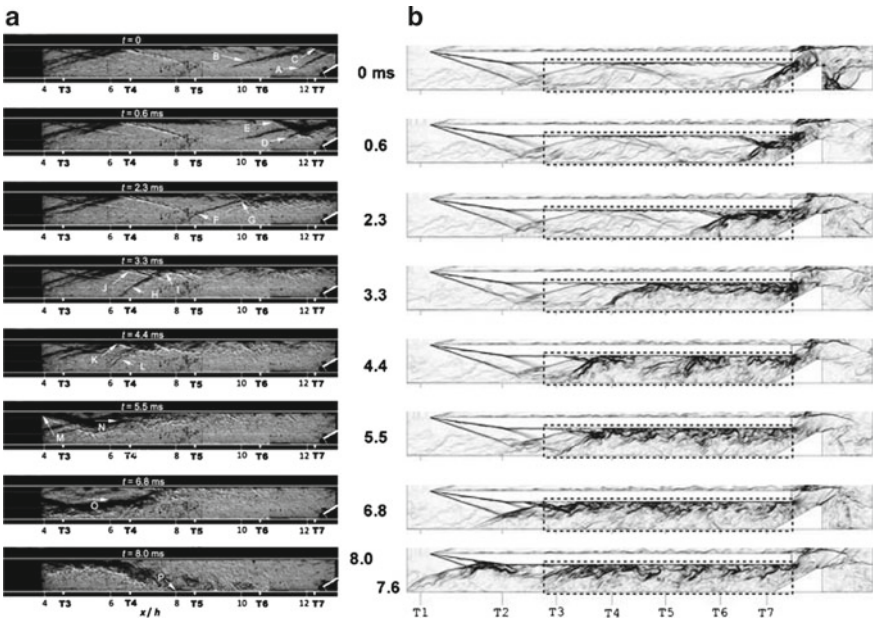

Fig. 1.10 **a** Experimental schlieren images and **b** density-gradient magnitude images from LES computations at corresponding scaled time for the 8 deg inlet unstart case. Experimental measurements are available corresponding to the boxed area in **b** [29]

the external unstart shock, they observed two kinds of secondary oscillations with high dominant frequencies of about 360 and 900–1300 Hz. It was found that these two secondary oscillations were both acoustic resonance modes formed in different parts of the duct.

Geerts et al. [32, 33] used background oriented schlieren (BOS) to study the shock train movement under slowly varying backpressure conditions in a rectangular isolator with Mach 2.5 upstream flow. It was observed that throughout the unstart process, the shock system behaved apparently oscillatory nature. Bruce et al. [34] studied a transonic duct with parallel walls at Ma 1.4, low-frequency downstream pressure perturbations (16–90 Hz) was enforced to the flowfield. It was concluded that the unsteady behaviors of relatively low frequency (40 Hz) could be captured well by the unsteady Reynolds-averaged Navier-Stokes scheme. However, the size of the interaction region was exaggerated by simulation. Bruce et al. [34] also found out that asymmetry existed in transonic channel flows, which was induced by the interaction of corner flows. Numerical simulations indicated that flowfield asymmetry occurred when the size of a corner interaction exceeds 35–40% of the channel width or height. Researches carried out by Su et al. [35, 36] focused on self-sustained and imposed oscillations of pseudoshock induced by back pressure. Their simulated results indicated that, an oscillation of 3107 Hz occurred when the ratio of backpressure to the

freestream static pressure reached 70. Li et al. [37] implemented wind tunnel experiments to investigate the oscillation characteristics of the shock train in an isolator at Mach 2.7, and a wedge was mounted upstream of the test section to generate incident shocks. It was found that an unsteadiness appeared when the leading edge of shock train was travelling through the SWTBLI region. This unsteadiness could be weakened by a faster backpressure rising rate. Xiong et al. [38] carried out several experiments to investigate the flow unsteadiness in a constant-area rectangular isolator. In self-excited oscillation, it was found that the low-frequency disturbance induced by the upstream shock foot motions could travel downstream and the frequency would be magnified by the separation bubble. In forced oscillation, results illustrated that the separation shock oscillation frequencies increased and the intermittent region lengths decreased with the increasing steady backpressure. Meanwhile, the amplitude of the shock train oscillation increased with the decreasing excitation frequency of the fluctuating backpressure. An analytical model [39] was developed based on the 'relative Mach number' mechanism and a quasi-steady assumption, which was able to predict the unsteady motion of shock train quite well.

Compared with inlets and isolators, unsteady separation of supersonic flow is more widely studied in nozzles. Since the supersonic nozzles resemble combustors in shape (expanded flow path), the systematic studies of unsteady separation in nozzles are especially heuristic.

Several researchers have been studying the asymmetric and unsteady separation phenomena in a supersonic nozzle for a long time. Typical flow behaviors and the mechanism of unsteadiness are revealed step by step. Reijasse et al. [40] made a preliminary study on shock-induced separation in a planar two-dimensional nozzle. With the rapid shadowgraph and three-dimensional laser doppler velocimetry method, they concluded that the flow field transferred from symmetric to asymmetric as throat contraction ratio increased, and returned to symmetric due to the further increase of throat contraction ratio. Yu et al. [41] discussed the switch of separation modes in an over-expanded single expansion ramp nozzle. Research showed that separation patterns changed between restricted shock separation and free shock separation during the startup process. Meanwhile, a shock wave instability [42] occurred during the separation transition phenomenon.

Papamoschou et al. [43, 44] found out that asymmetric separation occurred in a convergent-divergent nozzle which worked in over-expanded condition. Wall pressure measurements indicated that a low-frequency, piston-like unsteady shock motion exists without any resonant tones. Xiao et al. [45] used RANS to study the same nozzle as Papamoschou investigated, numerical results captured asymmetric separation under moderate NPR (nozzle pressure ratio) 1.6–2.3. Johnson et al. [46] made further study based on their previous work. They concluded that enhanced shear layer instability was strongly coupled to shock motion unsteadiness, while the wave pattern itself was not a cause of enhanced mixing. Olson et al. [47, 48] carried out LES simulation on the same case as Papamoschou and Johnson worked on. Based on directional artificial fluid properties method developed for wall-bounded flow, their simulation fully described the process of shock unsteady motions, as shown in Fig. 1.11. A reduced-order model was proposed based on the quasi 1d flow equations.

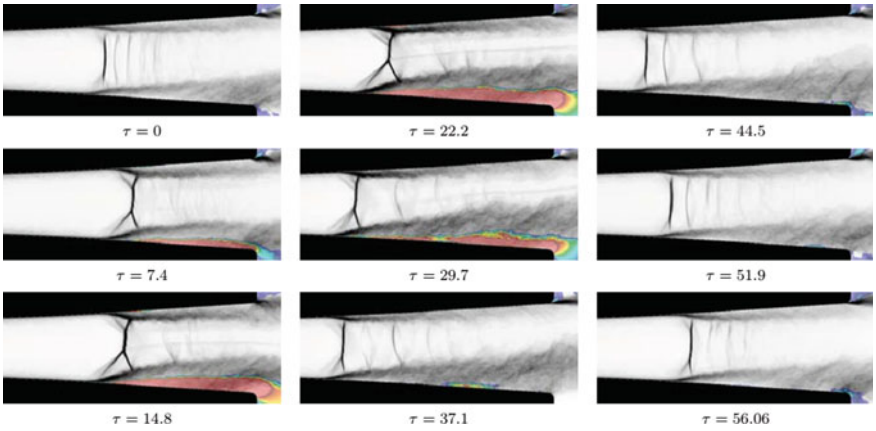

Fig. 1.11 Shock wave motion and the corresponding separated shear layer over one low-frequency process (Contours of $\|\nabla\rho\|$ are shown in grayscale and colored regions depict negative U velocity. Red represents a Mach number of approximately 0.1 and blue is 0) [48]

With systematic studies, their conclusions can be summed up as follows:

1 The asymmetry and unsteadiness of shock train become obvious when NPR is high, and the amplitude of oscillation is about half of the nozzle's height [43].
2 The shock foot and the shear layer of large separation side behave strong unsteadiness [49], which forms large vortices downstream. The shear layer at the other side develops at a normal rate. Such an unsteadiness is helpful in mixing enhancement.
3 The main component of oscillation is low frequency, which do not have an obvious peak. The back and forth motion of shock train results from shear layer instability, which has nothing to do with acoustic effects [50]. The oscillation is broadband, the high frequency component is controlled by the turbulent boundary layer and separated shear layer, while the low-frequency component is affected by shock intensity. Stronger shock leads to unsteady behavior more obvious [49].
4 Correlation analysis indicates that the total pressure of the shear layer at the large separation side has a positive correlation [46] with shock motion, which is opposite to normal one-dimensional shock theory.
5 Alternating wave pattern downstream the separation shock is not the main cause of unsteady process [46]. A wavy wall is implemented in the separate experiment to study the isolated effect of the alternating compression and expansion waves. Results suggest no increases in RMS pressure from both walls, which means the imposed wave pattern does not increase instability.
6 The source of the unsteady process probably results from the interaction of unsteady waves generated past the main separation shock with the shear layer of the large separation region [44], as shown in Fig. 1.12.

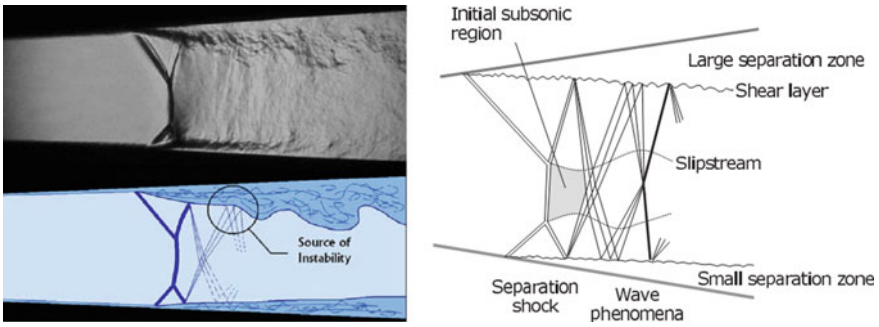

Fig. 1.12 Schematic of principal phenomena in supersonic nozzle flow separation [44]

1.2.3 Unsteady Combustion Dominated by Flow Instability

Unlike other parts, the flow dominating instabilities in combustor have not drawn enough attention. The separation induced unsteadiness in inlet and nozzle usually appears in off-design conditions (such as unstart and over-expanded). However, the large-scale separated region often exists in combustors which work under normal operating conditions (especially for high fuel equivalence ratio). Therefore, studying the separation-related phenomenon in supersonic combustor maybe even more important than the other parts of a scramjet. Moreover, due to the different configuration (converging inlet, constant-area isolator, and diverging combustor) and flow structures (normal shock train in the nozzle and oblique shock train in the combustor), the conclusions acquired from other parts of scramjet are probably problematic in combustors.

Up to now, only a few of researches have been focused on unsteady supersonic combustion processes which are dominated by flow instabilities. Laurence et al. [51] performed a series of experiments in the High Enthalpy Shock Tunnel Göttingen, in order to investigate the response of the HyShot II scramjet combustor to equivalence ratios close to the critical value at which the onset of thermal choking occurred. For the case with an equivalence ratio of 0.41, flow separated on the injector-side wall, which leads to the presence of large oscillations on the cowl-side wall. Based on the analysis from schlieren images, the high-frequency oscillation of shock train was observed. Fotia et al. [52] made contributions in searching out the mechanism of flame/shock-train interactions during the ram-scram transition. Under certain conditions of ramjet mode, they observed that some periodic low-frequency flame oscillations occurred. During the unsteady process, the oscillation of flame correlated well with pressure fluctuations. They concluded that the mechanism of flame oscillation was induced by a self-sustained shear-layer instability, associated with the flameholding cavity, as in Figs. 1.13 and 1.14. Yuan et al. [53] studied the flame stabilization characteristics in a dual-mode scramjet combustor with inflow Mach number of 2.5. It was found that the flame oscillated between the shear layer and the jet wake mode if the thermal

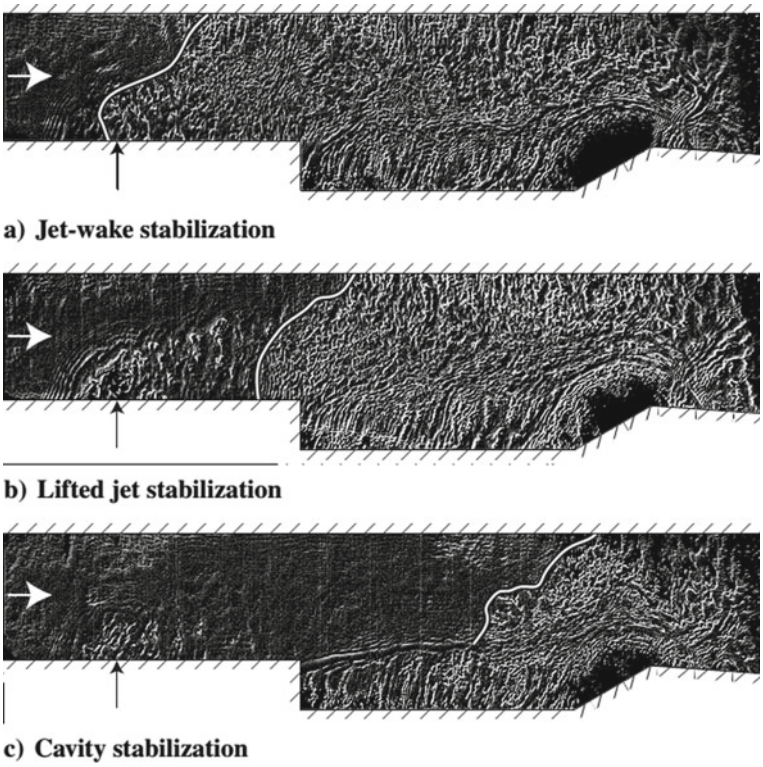

Fig. 1.13 Shearing interferograms of the **a** jet wake, **b** lifted jet, and **c** cavity flame stabilization modes in unsteady ramjet operation [52]

choke occurred around the injection location. They concluded that the short-lived aerodynamic throat was probably the cause of the flame oscillation.

Combustion is mainly affected by the mixing process when the combustor operates near the lean extinction limit. Instabilities accompanied by the flow features such as vortex, shear layer, shock wave, and boundary layer may strengthen the combustion unsteadiness. Flameholders and reasonable fuel injection patterns can improve combustion steadiness and make it more resistant to flow disturbances.

The flow in the combustor interacts with the combustion mainly through ignition and mixing processes. Therefore, stable combustion is often achieved by using recirculation zones to provide continuous sources of ignition, by well mixing the combustion products with fresh fuel and oxidant reactants [54]. Conventionally, swirl vanes [55], bluff-bodies [56, 57] and rearward-facing [58] steps are used as effective approaches to establish a recirculation zone for flame stabilization [55, 56, 58, 59]. These flameholders also introduce flow instabilities. In subsonic combustor, a bluff body could separate the incoming flow and develop shear layer instabilities. The alternating array of vortices shed from the trailing edge of the bluff body. These instabilities in most circumstances are responsible for initiating a blowout [60–62].

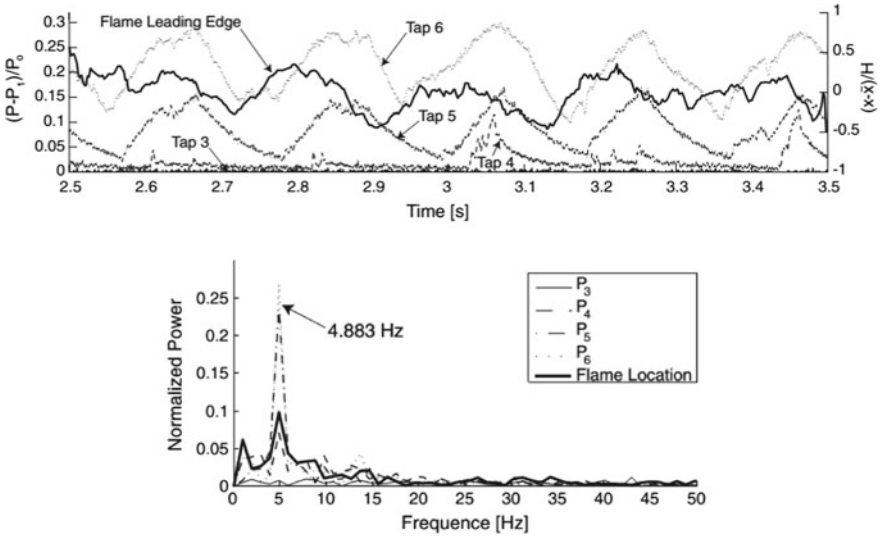

Fig. 1.14 Isolator shock-train static pressure traces (above) and spectra showing the dominant frequencies of the flame position and the pressure transducers (below) [52]

Gas turbines and aero-engines are used to apply swirl stabilizer to provide circulation zones [55, 63]. But the spinning speed of the swirler is limited to the velocity of coming flow. Considering the stringent NO_x emissions, industrial combustors must be operated near the lean extinction limit [64]. The combustion stability is more sensitive to the flow patterns.

Instead of aerodynamic features in swirl stabilizer, the trapped vortex combustor (TVC) uses geometric features to ignite the incoming fuel-air mixture and is less sensitive to unstable combustion [65, 66]. This concept was proposed by AFRL (Air Force Research Laboratory) in the 1990s or late 1980s [67] which is similar to the cavity used in scramjet. The conventional swirl-stabilized combustor and TVC are schematically shown in Fig. 1.15. A bluff or forebody is located upstream of a

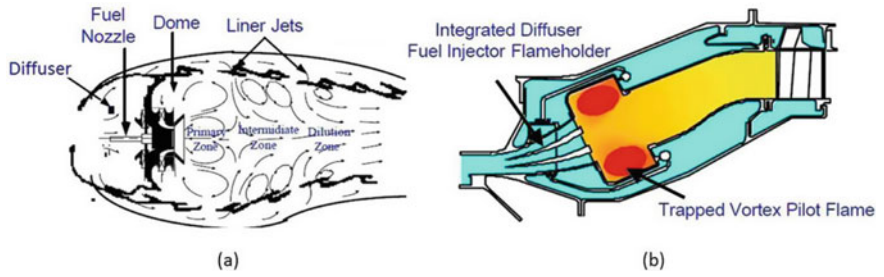

Fig. 1.15 Comparison between a conventional swirl-stabilized combustor and trapped vortex one. Adapted from Ref. [69]

smaller bluff body in TVC, and the vortices are trapped or locked between the two bodies [68].

In a TVC, air and fuel injection should be strategically-placed in the forward and rear walls of the cavity to drive the vortex contained. As the fuel is injected into the cavities, it is quickly mixed and burned in the stable trapped-vortex flow structure. The residence time of the supersonic and subsonic flow inside a cavity depends on the mass exchange rate in and out of the cavity. In the open cavities, mass and momentum transfer mechanisms are determined by the vortex structure inside the cavity and the longitudinal oscillations. Numerical results demonstrated [70] that there was one large vortex stationed near the trailing edge of the cavity and a secondary vortex near the upstream wall. The large trailing vortex interacts with the unstable shear layer and determines the mass exchange of the cavity. As the trailing edge vortex occupies a larger volume inside the cavity, the mass exchange is increased and the flow residence time inside the cavity is decreased. To minimize the combustion instability, the vortex must be "safely locked" in the cavity [71, 72].

There are also interests in whether spinning motion can improve the fuel-air mixing and combustion performance in TVCs. 3D streamlines in combusting flows with spinning motions are shown in Fig. 1.16a. Due to the swirling flows, strong tangential motion is introduced into the cavity vortex, and vortex breakdown is established in the sudden expansion region of the TVC. Turbulence kinetic energy and turbulence intensity are significantly increased. This indicates the fuel-air mixing can be dramatically improved. The spinning motion is found to lead to an increased combustion efficiency close to the spinning disc illustrated in Fig. 1.16b. And a study with a sudden change in swirl number is made. The transient results show that the cavity vortex is quite resistant to the flow disturbances. The vortex is trapped well in the cavity during the changing process.

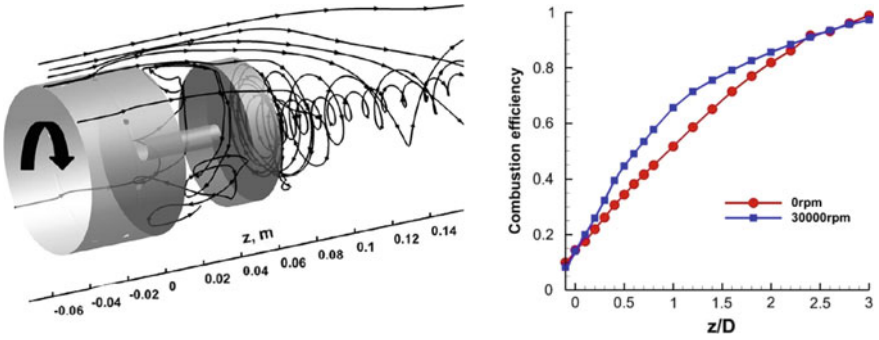

Fig. 1.16 3D streamlines of the combusting flows in the combustor: **a** 30,000 rpm, **b** Combustion efficiency for the non-spinning and spinning combustor [73]

1.2.4 Summary

Shock induced separation is a traditional problem in scramjet. Characteristic structures of reacting flow field are usually dominated by separation patterns when the heat release is strong enough. As the development of the experimental facility and computational capability, complex unsteady phenomena in non-reacting supersonic flow have been investigated by more and more researchers. The flow unsteadiness is believed to occur when the separation is severe, and is usually accompanied by asymmetric behaviors. The unsteadiness of separated flow is broadband, and main components of oscillation concentrate in the low-frequency band. Some studies suggest that interactions between separated shocks and shear layer instabilities account for the unsteadiness, while the majority of investigations only focus on the description of unsteady phenomena. It is believed that the unsteadiness in supersonic non-reacting flow has a strong relationship with the low-frequency unsteadiness in shock wave/boundary-layer interactions (SWBLI). Since the driving force for low-frequency unsteadiness in SWBLI is still controversial (upstream, downstream or combine), the cause of low-frequency oscillation in non-reacting flow remains not fully explained. In general, it is acknowledged that the downstream mechanism dominates for strongly separated SWBLI flows, and a combined mechanism (both upstream and downstream) dominates for weakly separated SWBLI flows. Meanwhile, the unsteadiness in supersonic combustion dominated by flow separation has not gained enough concern. Due to intrinsic complexities in shock wave/boundary-layer interactions, the unsteady combustion driven by back pressure induced separation is a challenging problem. Further studies are required to shed light on the unsteadiness of separation in reactive flows.

1.3 Ignition

Ignition is the beginning phase of combustion. The mechanism of the ignition process is widely investigated, and the effects of the parameters of the forced ignition system are clarified. In the scramjet combustor, the supersonic flow increases the difficulty of the ignition. Auto-ignition cloud also be induced with the high enthalpy flow. It changes the traditional ignition method and affects the combustion instability. Thus, the ignition process deserves extra attention.

1.3.1 Basic Concepts for the Forced Ignition

In low speed inflow conditions, the researches were concentrated on both spontaneous ignition (auto-ignition) and forced ignition (spark ignition). Many classical combustion articles have been widely reported. The technological applications in low speed

inflow conditions are closely related to our daily lives, such as spark ignition in gas turbines and auto-ignition in diesel engines. A classical formula of minimum ignition energy ($E_{\min}$) [74, 75] is proposed to calculate the minimum energy required for forced ignition, as seen in Eq. (1.3). In the equation, c_p is defined as specific heat at constant pressure, ρ is the gas density, ΔT is the temperature rise due to combustion and d_q is the diameter equal to the quenching distance.

$$E_{\min} = c_p \rho \Delta T \left(\frac{1}{6}\pi\right) d_q^3 \tag{1.3}$$

Under the conditions of low turbulence, the equation of minimum ignition energy is given as

$$E_{\min} = c_p \rho \Delta T \left(\frac{1}{6}\pi\right) \left[\frac{Ak}{c_p \rho (S_L - 0.16u')}\right]^3 \tag{1.4}$$

Under the conditions of high turbulence, the equation of minimum ignition energy is given as

$$E_{\min} = c_p \rho \Delta T \left(\frac{1}{6}\pi\right) \left[\frac{Bk}{c_p \rho (S_T - 0.63u')}\right]^3 \tag{1.5}$$

In Eq. (1.4), k is the thermal conductivity, S_L is the laminar burning velocity, S_T is the turbulent burning velocity, u' is the value of fluctuating velocity, A and B are constants. According to Eq. (1.5), it is concluded that the minimum ignition energy increases with the increase in the thermal diffusivity and turbulence intensity, and it decreases with the increase in density and burning velocity. When the turbulence level is high, they also proved that larger turbulence scale increases the quenching distance and causes a significant enhancement in the minimum ignition energy accordingly, which can be easily understood from Eq. (1.5) when u' increases much faster than S_T. Therefore, for the gaseous fuel ignition process, a much larger ignition energy is needed to achieve a successful ignition process under severe turbulent flow fields.

The equation of minimum ignition energy for liquid fuels [75] as

$$E_{\min} = \left[\frac{\left(\frac{1}{6}\pi\right) c_{p,a} \Delta T_{st} D^3}{\rho_a^{\frac{1}{2}}}\right] \left[\frac{\rho_f}{\phi \ln(1 + B_{st})}\right]^{\frac{3}{2}} \tag{1.6}$$

where $c_{p,a}$ and ρ_a are the above mentioned nomenclatures for air, ρ_f is the density of fuel, D is the droplet diameter, ΔT_{st} is the stoichiometry temperature rise, B_{st} is the stoichiometry mass transfer number, and ϕ is the equivalence ratio. From Eq. (1.6), it can be seen that the minimum ignition energy of liquid fuel is strongly influenced by the drop size, and to a less extent affected by the equivalence ratio and fuel density. As a result, fuel evaporation process is the key factor affecting the ignition of quiescent liquid fuels.

The above spark ignition model has been extended to include the effects of finite chemical reaction rates and the presence of fuel vapour in the mixture flowing into the ignition zone. In the new model, different mixtures were represented by using different quenching distance equations. The detailed modified minimum ignition energy equations could be referred to Ref. [76].

The most important concept of the ignition energy is the minimum ignition energy (MIE) which is widely studied in low speed flows. From these equations of minimum ignition energy discussed above, fundamental requirements of ignition energy can be known based on sample calculations and easily achieved in many industry related combustion operations. However, for the flame kernel needs much more energy to resist the severe turbulent dissipation, many ignition methods in supersonic flows could provide ignition energy much more than MIE during the ignition process. Therefore, MIE is less focused in supersonic flows whereas flame behaviors with different ignition energy are concentrated.

The biggest challenge for the ignition process is the flame propagation at the initial ignition phase, which is highly affected by the fuel/air mixing as well as the turbulent flow field. During the past decades, effects have been gained on investigating the ignition flame propagation process, and it is found that turbulent-chemistry interactions are of vital importance to the above process. Considering the complexity of turbulent-chemistry interactions, however, accurate flame propagation models are rarely reported. Mastorakos [77] did comprehensive reviews on both the auto-ignition and the spark ignition processes in turbulent non-premixed flames under low speed inflow conditions and emphasized fundamental turbulent-chemistry interactions. Detailed descriptions about the research progress on the turbulent-chemistry interactions during ignition process can be referred to their research.

1.3.2 Effects of the Forced Ignition Methods

In a cavity-based scramjet combustor under a supersonic inflow condition, the inflow velocity is typically over 1000 m/s and the recirculation flow velocity inside the cavity is varied from approximately 0–200 m/s [78]. The velocity gradient from inside the cavity to the core flow brings a significant challenge to the flame propagation, which is likely to extinguish the weak flame during the initial ignition phase. It can be indicated that a much severe turbulent dissipation will occur during the ignition process in the supersonic flow. On the other hand, the stagnation temperature of the supersonic flow (such as, over 1500 K in Mach 6 condition and over 800 K in Mach 4 condition) is much higher than that of the atmosphere. The static temperature of the recirculation flow inside the cavity under supersonic inflow conditions is also estimated over about 700 K [79], which in turn creates a more chemical friendly environment. Thus, the turbulent-chemistry interactions of the cavity ignition process will be much more complicated than that reviewed by Mastorakos [77]. Nevertheless, considering the complex flow phenomenon occurring in supersonic flows, such as the fuel/air mixing, boundary layer separation and air stream shearing, the cavity ignition becomes a

much more complicated physical process. As a result, much harder predicted ignition probability and more complex influencing factors are presented in the cavity ignition process in supersonic flows, leading to a relatively slow research progress in the supersonic research fields during the past decades.

As mentioned in the open literature, many new ignition methods have been developed to achieve successful cavity ignition in a supersonic flow, however, the most widely used igniter is still the spark ignition system. Although the spark plug is widely applied in our daily life, the mechanism of the spark ignition process is still complex and rarely focused especially in a supersonic flow. McNeil [80] studied the ignition process by electrical sparks and classified the spark ignition process into five stages as breakdown, electron heating, relaxation of internal plasma energy, shock wave generation and propagation, and subsonic flows. Brieschenk et al. [81, 82] conducted an experimental investigation of a capacitive-discharge spark ignition system in a cavity based combustor by utilizing Schlieren and luminescence imaging techniques in a Mach 6.6 flight condition. In their study, three ignition coils were compared with different spark plug gaps in order to evaluate the ethylene ignition performance and it was demonstrated that the spark plug gap is a vital factor affecting the ignition process. It was found that the ignition system parameters can be set to cause sufficient heating of the electrodes to obtain a successful ignition. Denman et al. [83] also applied spark plug to test a cavity flameholder in a Mach 8 shock tunnel. In their experiments, successful ignition and flameholding of ethylene and hydrogen were observed at an equivalence ratio ranging from 0.58 to 0.71. Although the inflow Mach number is relatively high with a favorable chemical reaction temperature, however, methane did not ignite at any tests. The spark ignition is mainly used in igniting gaseous hydrocarbon fuels under supersonic conditions. Spark ignition in liquid kerosene fueling cavity is rarely reported without the aid of other methods. The reason causing the above limitation is the shortage of spark ignition energy.

Pulse detonation igniter is recently developed and proved favorable for the ignition process in supersonic flows. Compared to spark discharge providing a small pure electrical energy addition for ignition, the pulse detonation provides a chemical heat release technique with a high pressure, temperature and radical-rich plume. Besides, detonation is a superior combustion form owing to the coupling between the shock and flame front which can provide rapid heat release and elevated pressure. Ombrello et al. [84, 85] did comprehensive and frontier investigations on the pulse detonation ignition method, and their pulse detonation igniter system is shown in Fig. 1.17. They selected propane (C_3H_8) and nitrous oxide (N_2O) as the fuel and oxidizer, respectively, because of their reliability of igniting and transitioning to detonation under the conditions needed for the experiments. They studied the cavity ignition processes in a supersonic flow by using two different ignition method, spark discharge and pulse detonation, and also discussed the effects of inflow distortion and mixing enhancement on the above ignition processes [84, 86]. Compared to the spark discharge, the pulse detonation can create an environment with a higher pressure and temperature which not only broaden the ignition limits but also cause a significant disruption to the cavity flow field. In addition, they emphasized the importance of cavity flow field

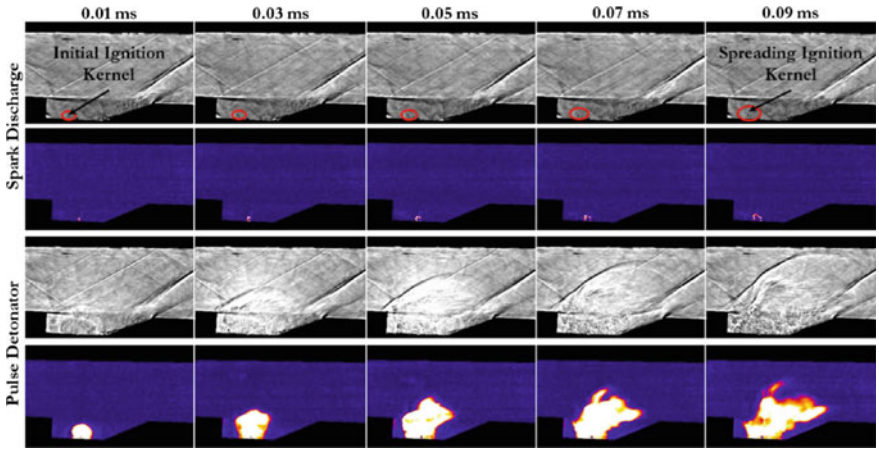

Fig. 1.17 Shadowgraph and CH* chemiluminescence images of cavity ignition processes excited by spark discharge and pulse detonation, respectively [84]

dynamics and fueling rate for a successful ignition. Recently, they applied simultaneous 100 kHz formaldehyde planar laser-induced fluorescence imaging in combination with CH* chemiluminescence imaging to investigate the transient ignition process in a cavity-based supersonic combustor. According to their research, it was indicated that there exists a strong correlation between the delay time from the onset of ignition to flame stabilization and the cavity fueling rate [87]. Furthermore, they studied the ignition mechanisms involved in transferring a detonation to a deflagrating scramjet cavity by clarifying the decoupling process of the detonation recently [88]. They proved that the shedding of high-temperature intermediate species is the primary mechanism governing successful ignition in the scramjet cavity. The pulse detonation is a promising ignition method with adequate ignition energy, and it will be more practical after decreasing the size of the igniter as well as the detonation fuel delivery system.

In the fields of cavity laser induced plasma (LIP) ignition, Yang et al. [89–91] performed a lot of experiments in hydrocarbon fueled cavity based scramjets in Mach 6 flight conditions. They applied LIP method to investigate single-pulse ignition [90], dual-pulse ignition [92], dual-point ignition [93] and also ignition mechanisms [94, 95]. According to their research, the energy of an individual laser pulse can be reduced by half via a dual-pulse LIP method as compared with a single-pulse LIP with the same total energy. Besides, a pulse interval shorter than 40 μs is suggested for dual-pulse LIP method. Even though they tried dual-point LIP ignition method, it is not suggested to apply in a real scramjet combustor owing to significant radical loss and heat loss as a result of spatial distribution of the plasma by dual-point LIP method. They revealed that the ignition process can be characterized into four stages: an initial plasma ignition stage, followed by the plasma-quenching stage, the re-ignition stage, finally, the stable flame stage. Despite detailed experimental

observations mentioned above, numerical simulations were also performed to further study the mathematical model of dual-pulse laser ignition [96] and also the ignition process [97]. The significant advantages of LIP to other ignition methods are precisely controlled excitation energy, frequency as well as ignition location. In addition, it won't cause any disturbance to the flow field due to its non-intrusive characteristics. In the current LIP applications, laser system is rather big which is only suitable to use in a lab. In the future, LIP ignition method will become more and more practical after minimizing the laser system.

Electrical discharge ignition method is proposed to enhance the ignition ability of spark discharge and it belongs to the plasma-assisted ignition. In addition, the concept of plasma-assisted ignition not only includes ignition acceleration, but also the mixing enhancement and flame stabilization. Firsov et al. [98] conducted optimization of electrical discharge (10 kW) geometry in a Mach 2 supersonic inflow. It was reported the combined mixing/ignition geometry in which plasma penetrates into the fuel injector demonstrates a significant advantage in terms of ignition and flameholding. They also conducted experimental and numerical study on long spark plasma actuator for mixing enhancement in a supersonic flow [99]. It was demonstrated that there exists a strong correlation of jet instability with a local curvature of the discharge channel and the long spark discharge stretches the interface between fuel jets and supersonic inflow [100]. Savelkin et al. [101] investigated the ignition and flame stabilization processes in a Mach 2 supersonic inflow by an electrical discharge combined with an ethylene injector. In their study, a wall-fuel injector and a high-voltage electric discharge were installed into a single module, which demonstrated a significant advantage in terms of ignition and flameholding limits. Recently, Leonov et al. [102] conducted experiments to further study the ethylene ignition and flame stabilization by electrical discharge (15.7 kW) in a scramjet combustor and explored the sensitivity of the ignition dynamics to the plasma power. In the field of plasma-assisted ignition caused by electrical discharge, gliding arc plasma is also recognized to expand ignition and extinction limit with low energy consumption in the recent years. Wu et al. [103] experimentally demonstrated that gliding arc plasma (2 kW) could achieve combustion enhancement in a cavity based scramjet due to heating and chemical effects. In their study, it was concluded that the ignition limit is nearly equal to the blow-off limit of ethylene flame owing to the gliding arc. To achieve reliable and fast ignition in the scramjet combustor, Wu et al. [104] also proposed multichannel plasma igniter (MCPI) to induce a relatively larger ignition kernel at the beginning phase. They reported that the lean ignition limit of ethylene flame in a scramjet combustor through MCPI is expanded by 20–26% than that through spark ignition and the ignition time is reduced by about 50%.

To achieve a successful ignition in the scramjet engine, one of the ignition aids which is known as air throttling is to modulate the flow structures in the isolator and combustor in order to reduce the local flow velocity and increase the pressure, then the established shock train can facilitate ignition and flame stabilization. Li et al. [105] did comprehensive studies regarding air throttling ignition in an ethylene fueled scramjet combustor at flight Mach 5 condition. In their experiments, air throttling is activated after the cavity fueling is steady and the igniter is turned on. After

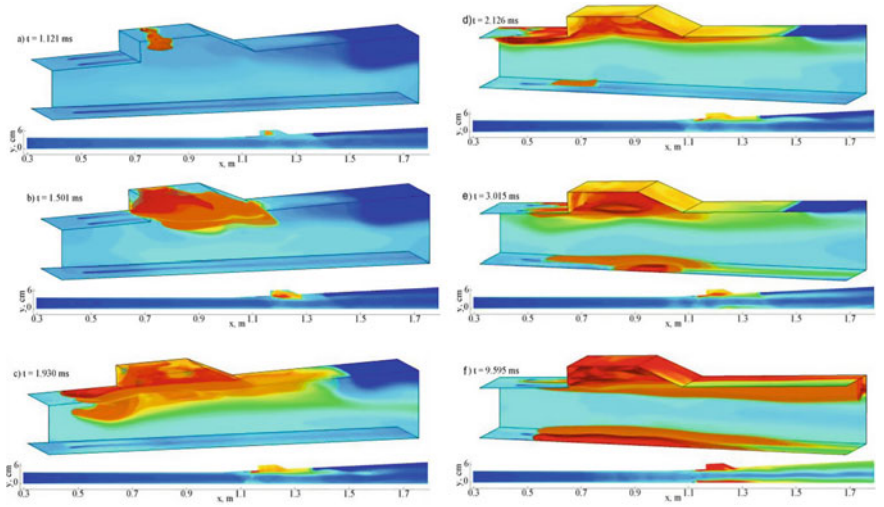

Fig. 1.18 Evolution of the temperature field in the cavity region during the ignition transient on the bodyside wall with air throttling ($\dot{m}_{throttle} = 20\%\ \dot{m}_{air}$) [106]

flame stabilization is achieved in the combustor, air throttling is then terminated to minimize the total pressure loss of the core supersonic flow. They numerically investigated the non-reacting and reacting flows during the air throttling working process [79, 89]. It was found that chemical reactions are intensified which produce sufficient heat release to maintain a flow environment conducive to flame stabilization. The temperature distribution is given in Fig. 1.18. As a result, a self-sustaining mechanism is established between the flow and flame development, and flame stabilization is achieved in the combustor even after the deactivation of air throttling [106]. In addition, they also studied control and optimization issues of the air throttling ignition process based on quasi-one-dimensional analysis, and a parametric investigation was conducted [107]. Noh et al. [108] numerically studied the auto-ignition process in an ethylene fueled cavity based combustor with air throttling. It was shown that air throttling increases the flow temperature and pressure as well as mixing enhancement in the pre-combustion region, which greatly improves the ignition efficiency and leads to a stable flame. Yang et al. [109] and Tian et al. [110] also conducted both numerical and experimental studies on the air throttling process in a kerosene fueled cavity based dual-mode scramjet combustor. They found that the combustion mode would change from supersonic combustion to subsonic combustion with throttling air injected into the combustor. The mode transition is mainly affected by the mass flow rate of throttling air and the throttling-off time [111]. They also classified the combustion into different parts to further study the mechanism controlling the air throttling process [112].

Obviously, self-ignition method is not suitable to work at low flight Mach number condition, and it still needs another igniter system to initiate the combustion of

vaporized kerosene at high flight Mach number condition. It is also not favorable for the real scramjet applications.

Representative investigations of the above ignition methods discussed in this section are summarized as listed in Table 1.1, which presents recent research progress on the cavity ignition field. It is obvious that the ignition methods with consistent and newest concentration are pulse detonation, laser-induced plasma, electrical discharge and air throttling ignition methods. The advanced optical observation measurements as well as detailed simulations are conducted in these investigations. In addition, it is also indicated that the research routine is changed from experimental tests discussions in the early 2000s to detailed reacting flow field analysis nowadays with the aid of the development of experimental and numerical measurements. From the practical point of view, however, only laser-induced plasma and air throttling ignition methods of the above four are of real interest to the future scramjet applications owing to reported successful kerosene ignitions as listed in Table 1.1. Meanwhile, all the other ignition methods are still of great significance to understand the complex cavity ignition mechanism.

1.3.3 Effects of Auto-Ignition

The auto-ignition is expected to occur at high stagnation temperature conditions when the order of the ignition delay time is less than the order of the flow residence time in real scramjet operations.

Since flame propagation has significant influences on the supersonic combustion, it is difficult to clarify the effects of auto-ignition. Fureby et al. [122] investigated hydrogen-vitiated-air flames with two stage and alternating-wedge injection struts. The temperature of vitiated air was 830 K with Mach number 2.5 in the combustor. The combustion region is consisted of auto-ignition zones enfolded by self-igniting fronts embedded in the background of non-premixed flames. By introducing planar laser-induced fluorescence (PLIF) of OH and CH_2O, auto-ignition is observed in a jet flame with a vitiated co-flow of 1355 K by Gordon et al. [123]. Cabra [124] experimentally studied a lifted methane-air jet flame in a vitiated co-flow with total temperature of 1350 K, and Domingo et al. [125, 126] suggested that in the experiment, the turbulent flame base began with auto-ignition to provide the every first ignition point. When the temperature of co-flow air is 1550 K, Yoo et al. [127] suggested that auto-ignition provides every first ignition point in the turbulent flame base. Lu et al. [128] indicated that auto-ignition could be the controlling factor determining the lifted-off height under the temperature of 1150 K.

The unsteady phenomena are more complicated in the transverse jets. Turbulent structures carry fluid packets that are further broken down for efficient mixing. Shock wave discontinuities and their interactions with the boundary layer and recirculation zones create distinct regions of different mixing qualities. It increases the difficulty to investigate the effects of auto-ignition. Both auto-ignition and thickened flamelets were observed by Micka et al. [129, 130]. As shown in Fig. 1.19, a strong

Table 1.1 Information for the cavity ignition methods in partial literature

Authors	Ignition method	Technique	Inflow Mach number	Year	ER
Sun et al. [113]	Spark	Schlieren; high speed photography	1.92	2012	Hydrogen; 0.17, 0.34
Denman et al. [83]	Spark	Wall-pressure measurement; RANS	3.0–5.0	2016	Ethylene, hydrogen; 0.58–0.71
Ombrello et al. [87, 88]	Pulse detonation	Formaldehyde PLIF (100 kHz); Schlieren; CH* chemiluminescence	2.0	2017, 2018	Ethylene; 0.5–1.5
Yang et al. [90, 95]	Laser-induce plasma	CH* and OH* chemiluminescence	2.92	2018, 2017	Ethylene, 0.15; Kerosene, 0.23
Brieschenk et al. [81, 82]	Laser-induce plasma	PLIF; Schlieren	5.7	2014, 2013	Hydrogen
Leonov et al. [102]	Electrical discharge	Schlieren; High speed photography	2.0	2018	Ethylene; 0–0.2
Savelkin et al. [101]	Electrical discharge	Schlieren; High speed photography	2.0	2015	Ethylene; 0–0.16
Kim et al. [114]	Plasma torch	Schlieren; Wall-pressure measurement	2.0	2011	Hydrogen; 0–0.1
Matsubara et al. [115, 116]	Plasma torch	Wall-pressure measurement	1.0, 2.0, 2.5	2011, 2013	Hydrogen; 0.06
Li et al. [79, 89]	Air throttling	RANS	2.2	2015	Ethylene; 0.6
Tian et al. [110–112]	Air throttling	RANS; Schlieren; Wall-pressure measurement	2.0	2015–2017	Kerosene; 0.3, 0.6, 0.8
Xi et al. [117]	Piloted	Schlieren; High speed photography	2.52	2014	Kerosene (piloted ethylene)
Situ et al. [118, 119]	Hot jet	Photography; Wall-pressure measurement	2.15	2001, 2002	Kerosene; 1.11–1.51
Li et al. [120]	Hot jet	High speed photography; RANS	1.92	2012	Kerosene; 0.3, 0.5
Sung et al. [121]	Self	Wall-pressure measurement	2.5	1999	Hydrogen; 0.6

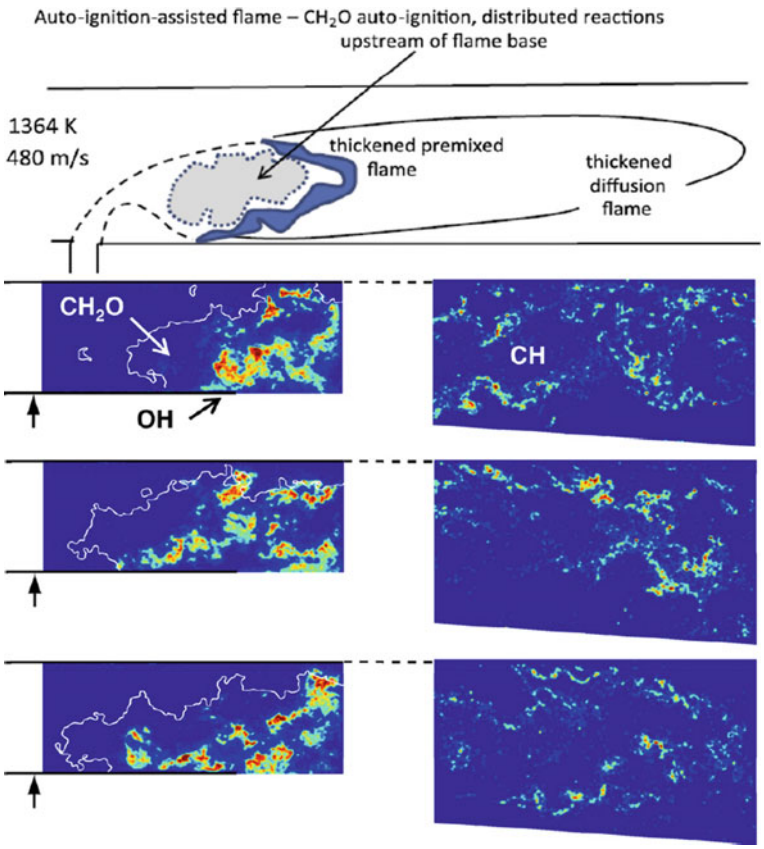

Fig. 1.19 Simultaneous formaldehyde-OH PLIF images [130]

formaldehyde signal was distributed in the lift-off region indicated that auto-ignition was presented. The auto-ignition existed upstream of the major heat release zone identified by OH signal, indicating the auto-ignition effected the flame base. They suggested that the combustion could be classified to an "auto-ignition assisted flame" under stagnation temperature of 1450 K.

Wang et al. [131] further reported that the flame front could be partially affected by the auto-ignition process of the combustible structure formed around the jet mixing layer. Under a very high stagnation temperature of 3750 K, auto-ignition was observed close to the bow shock, and combustion was a mixing-limited process mainly affected by auto-ignition [65].

1.3.4 Summary

Basic concepts for the forced ignition was introduced, and the widely used ignition methods in the scramjet combustor were provided in this section. The ignition process will be enhanced obviously with an increased ignition energy. Besides, the ignition method and the ignition location could affect the flame behaviors. When the flight Mach number increases, auto-ignition becomes significant, effecting the ignition phase and the combustion process. It provides the flame base and determines the lifted-off height and the flame may be stabilized as "auto-ignition assisted flame".

1.4 Flame Flashback

Flashback is the condition of the flame propagating down the hoses of an oxy-fuel welding and cutting system. The flame burns backwards into the hose, causing a popping or squealing noise, which affects combustion both in internal combustion engines and ramjets.

A number of studies [131–135] have been carried out concerning fuel injection and mixing with air, in order to burn completely within a short time. Transient flame flashback which is an indispensable key sub-process of combustion oscillation have been neglected for a long time because of the general thought that acoustic waves cannot propagate upstream in supersonic flowfield, and any flow oscillation resulting from an unsteady combustion process will be simply exhausted from the engine exit and will not interact with the flame zone [11, 12]. The first study to systematically investigate flashback limits is that of Lewis and von Elbe [136], whose model has remained as the state of the art for order-of-magnitude flashback predictions.

The existence of unsteady combustion process has been unfolded by many experiments. So far, the following reasons, such as DDT (deflagration–detonation transition) [134, 137], auto-ignition [138, 139], boundary layer separation [14, 140–142], and thermal choking [52, 143–146], have been considered responsible for the combustion oscillation in scramjet by different researchers.

1.4.1 Flashback Due to DDT (Deflagration–Detonation Transition)

When the fuel injection upstream of the cavity flameholder produces a premixed region with sufficiently high global equivalence ratio, a rapid flame flashback occurs against the incoming supersonic flow. The flashback develops explosively from the cavity pilot flame at regular intervals. Analysis of the experimental data suggests that the flame flashback is related to flame acceleration similar to deflagration-to-detonation transition. With high equivalence ratio, the immediate flame re-ignition

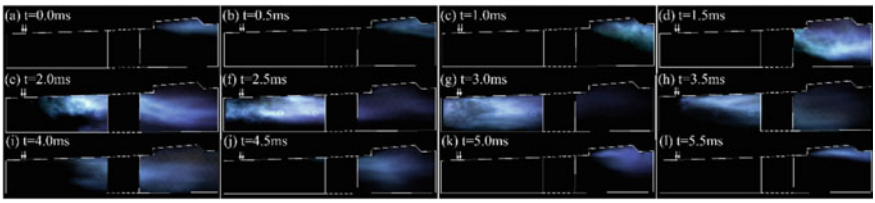

Fig. 1.20 Typical luminosity movie of flame flash-forward and blow-off event between cavity stabilized location and injection location [134]

and intense flame flashback decreases the flame blow off duration and finally leads to a more efficient heat release compared to the cases with lower equivalence ratio [132]. Many experiments shows that the flashback is caused by DDT (deflagration–detonation transition) [134, 147, 148]. O'Byrne et al. [140] also observed the flame flashback phenomenon, which is attributed to transition from diffusive to pre-mixed combustion. Aiming to compare the combustion stabilities of various mixing conditions, Wang et al. [134] designed several different injection schemes to investigate combustion instabilities inside an ethylene-fueled scramjet combustor. Figure 1.20 shows the high-speed flame luminosity images of the combustion oscillations. The images demonstrate the details of a flame flash-forward (from C0 cavity to I31 injection location) and flash-back. From Fig. 1.20d–g it is seen that the propagation of the flame from the cavity to the fuel jet occurs in the main flow, not just in the boundary layer. The flame base moves forward very quickly (Fig. 1.20c–e) until it reaches the fuel jet location (Fig. 1.20f).

Zhu et al. [149] investigated flame stabilization and propagation inside a kerosene-fueled two-stage strut dual-mode scramjet combustor experimentally, as shown in Fig. 1.21. The flame flashback equivalence ratio is much higher than the flame blowout limit, and the upstream strut can get a stabilized flame once it is reignited. A higher stagnation temperature and a lower inflow Mach number are advantageous to trigger flame flashback.

1.4.2 Flashback Due to Boundary Layer Separation

As previous references show [14, 140–142], the boundary layer separation can lead to the flame flashback. Usually, a disturbance is observed to upstream. This disturbance is interpreted as being due to separation of the boundary layers caused by the adverse pressure gradient to which the boundary layers are subjected. The separation reduces the effective flow area, thereby restricting the flow and pushing a shock (or shock trains) upstream to eventually unstart the duct [14]. Detailed shadowgraph images showed that the injection behind the pylon removed all the liquid from the wall surface, which is important for the elimination of potential flashback. These studies indicated that addition of fuel either in the inlet or in the scramjet's isolator

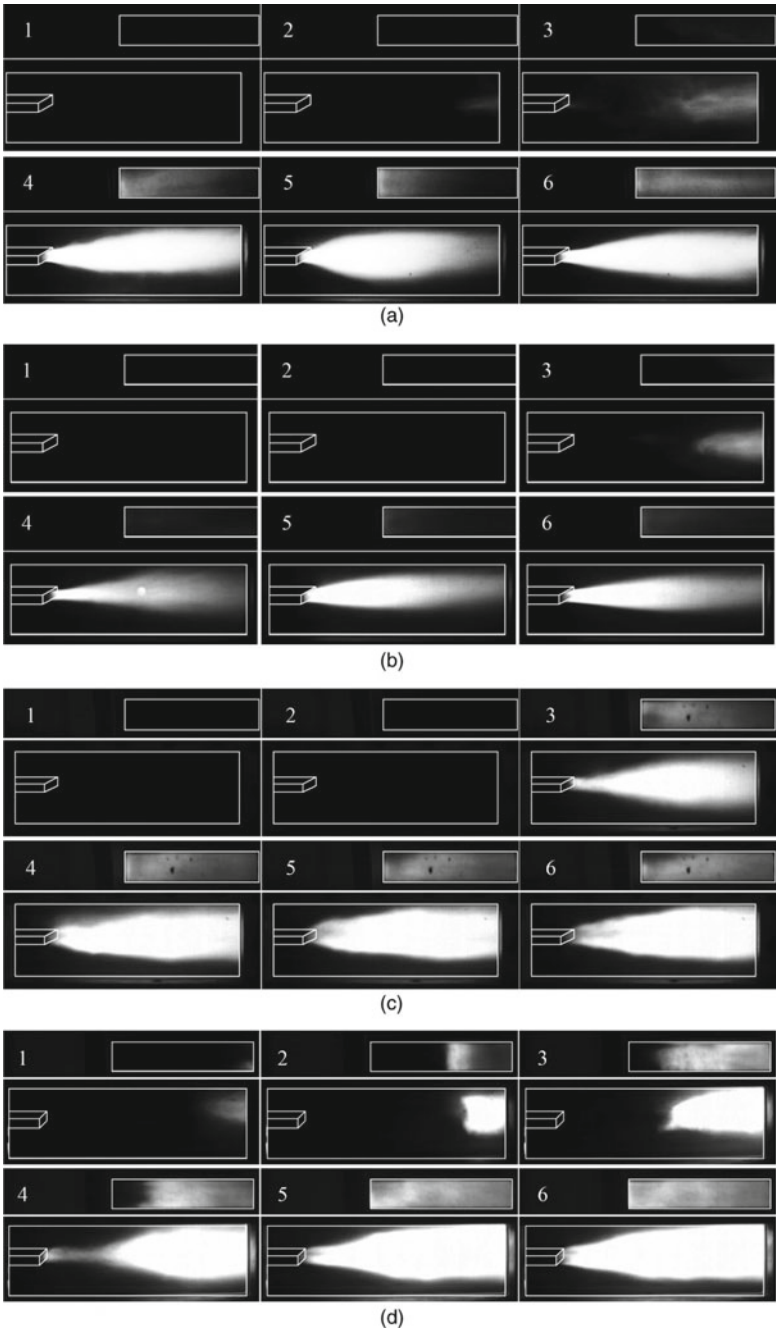

Fig. 1.21 Flame flashback captured near the upstream strut [149]

led to enhanced efficiency of the combustor operation. Flashback or inlet unstart can be avoided if careful consideration is given to fuel penetration, residence time, operational conditions, and fuel physicochemical properties. The main results indicated that thin pylons with sharp leading edges do not introduce significant pressure losses or flow distortion in the isolator airflow, but they create a region of low pressure, which has a great impact on fuel penetration. Even at moderate dynamic pressure ratios, the presence of these pylons promotes substantially higher penetration in comparison with simple wall injection. Because of this increased penetration, the entire liquid jet is lifted from the wall, eliminating the danger of flashback through seeding of the boundary layers with a combustible mixture [142].

Ducruix et al. [3] experimentally explored the combustion oscillation mechanism and control methods in an air-breathing engine. They found processes involving acoustic/flame coupling, unsteady strain rates, flame response to inhomogeneities, interactions of flames with boundaries, and flame/vortex interactions. Tian et al. [112] and Yang et al. [109, 150] found an intensive combustion in the whole cavity and wall boundary layer could be achieved with a careful air throttling method, or else leading to the combustion oscillation. The two processes might interact with each other, which would render the oscillations more complicated. As Fig. 1.22 shows, the shock waves kept moving upstream from the cavity region into the isolator, and then the flame near the cavity ramp propagated upstream along the cavity wall.

The investigations of Gruber et al. [151], which involved high-resolution experimental measurements and direct numerical simulations, focused on the characterisation of flame flashback for premixed and preheated hydrogenated flames in turbulent boundary layers. Those researchers showed that the near-wall speed fluctuation pattern found in turbulent boundary layers causes wrinkling of the initially flat flame sheet as it starts propagating against the direction of main flow, and that the structure of the characteristic streaks of the turbulent boundary layer has an important impact on the resulting flame shape and its propagation mechanism. They also indicated that flame flashback should be attributed to thermal choking, which is caused by downstream combustion and an adverse pressure gradient.

Figure 1.23 illustrates several stages of the unsteady flame propagation along the channel walls. The surfaces visualized represent:

(i) the streamwise velocity normalized by the friction velocity $u^+ = u/u_\tau$ on the $y^+ = 5$ plane (greyscale flooded contours on the plane parallel to the wall);
(ii) the wall-normal vorticity ω_y on the $y^+ = 5$ plane denoting the streamwise vorticity structures of the boundary layer (white lines on the plane parallel to the wall, solid and dashed lines denote opposite sign);
(iii) the flame surface as described by the progress variable isosurface, $C = 0.7$ (red isosurface);
(iv) back-flow regions characterized by negative streamwise velocity and located upstream of the flame surface portions that are convex towards the reactants (blue isosurfaces).

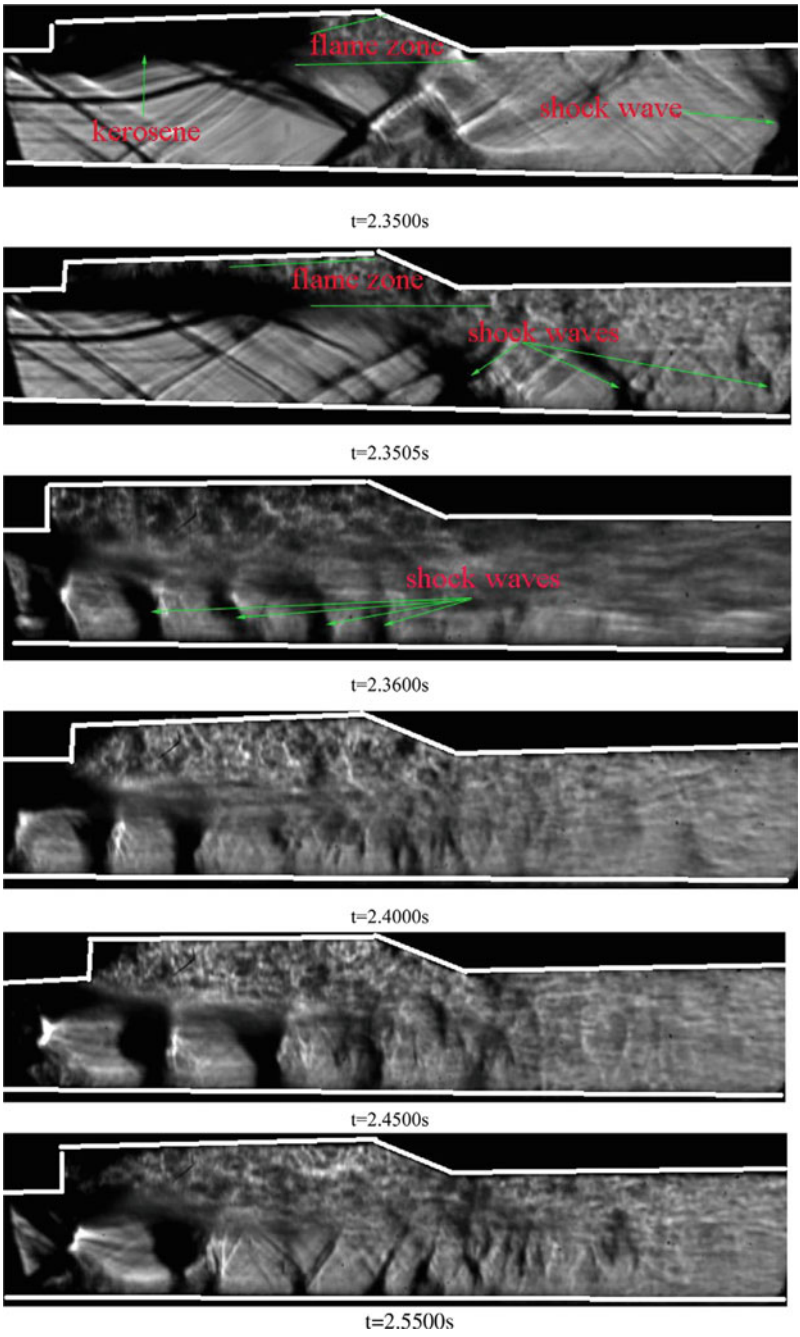

Fig. 1.22 The high-speed schlieren images of part-c and part-d combustion process [112]

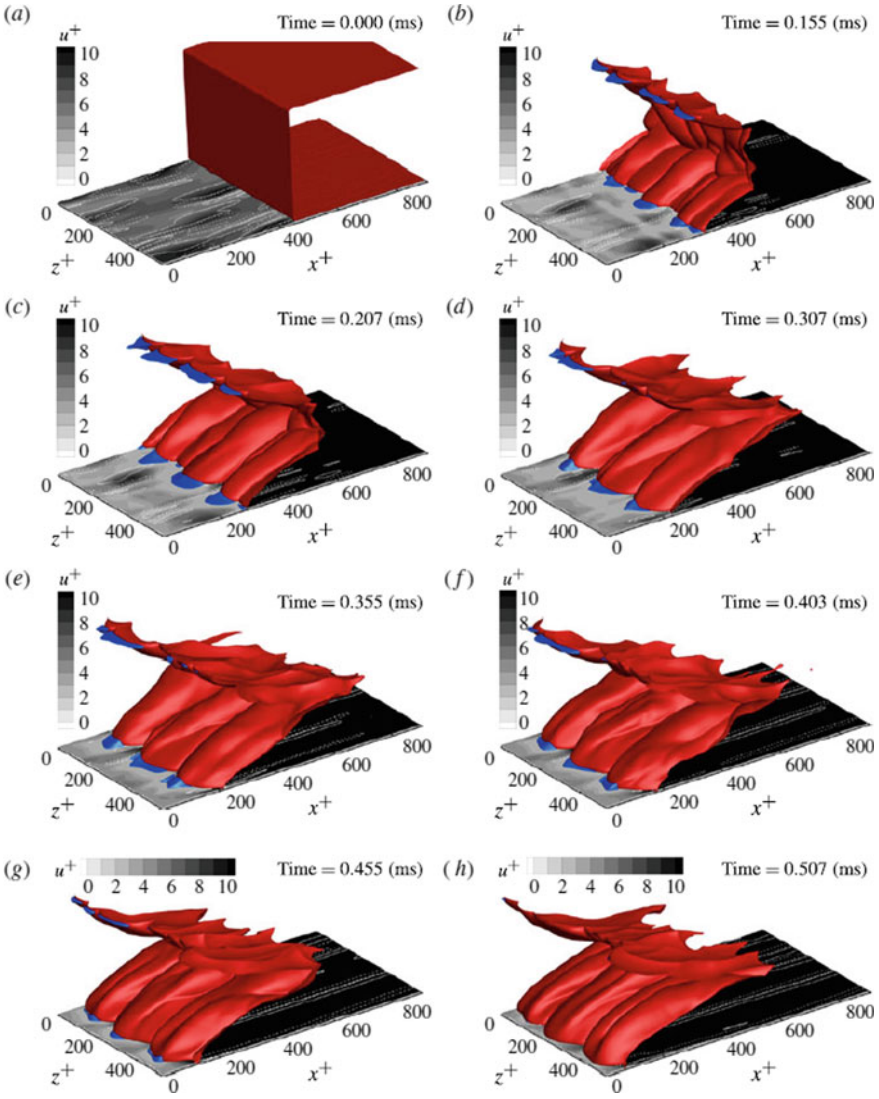

Fig. 1.23 Temporal evolution of the premixed flame (C = 0.7), red isosurface, and of the backflow regions, blue isosurfaces, from the beginning to the end of the reactive simulation. The non-dimensional streamwise velocity (greyscale flooded contours) is shown on the $y^+ = 0.5$ plane together with the trace of Y vorticity (white lines, solid and dashed patterns represent opposite sign) [151]

1.4.3 Flashback Due to Thermal Choking and Acoustic Instabilities

Thermal choking [52, 143–146] have been considered responsible for the combustion oscillation in scramjet. Larsson et al. [144] numerically investigated the mechanism of thermal choking using large eddy simulations (LES). The first objective of their study is to predict the pressure-rise in the combustor, which is within the experimental bounds, and shows reasonable grid-convergence. The second objective is to study the flow for increased fuel/air equivalence ratios. They also estimated the effect on the overall combustor performance. Karl et al. [145] focused on the numerical investigations of unsteady phenomena at large equivalence ratios. The main result was that the combustion efficiency decreases with an increasing fuel mass flow rate which coincides with significant flow separation. In the past decades, the effects of fueling schemes on the combustion stability characteristics in scramjet combustor equipping cavity flame holders have been studied widely. For high fuel-equivalence ratios, however, the flame base or combustion zone might be pushed upstream of the cavity intermittently due to the large separation of the upstream boundary layer and enlarged cavity recirculation, resulting from the intense heat release around the cavity and the interaction between the jet and the cavity shear layer. Laurence et al. [143] concluded that the primary mechanism responsible for the development of the transient shock system is thermal choking by OH* visualizations (as Fig. 1.24 shows) and numerical simulations. OH* visualizations did not indicate the presence of strong separation features propagating upstream with the shock train near its point of formation, suggesting that the driving mechanism for the transient development was thermal choking. Nevertheless, boundary-layer separation was observed to develop on the injector-side wall when the shock train had moved further upstream.

Lin et al. [13] studied the relationship between thermo-acoustic instabilities and the flame flashback. In addition, Ma et al. [11] obtain the mechanism responsible for driving the flow oscillation was identified as the acoustic-convective. The details are introduced in chapter 1.1.3. Rossiter et al. [152] developed semi-empirical formula to predict the resonant frequency of the compressible flow-induced cavity oscillation based on the coupling between the acoustic radiation and the vortex shedding.

1.4.4 Summary

There are several factors which causes flame flashback under different conditions, including DDT (deflagration–detonation transition), boundary layer separation, and thermal choking and acoustic instabilities.

Despite all the investigations performed, the physical mechanisms of the low-frequency oscillations in scramjet engines remain unclear. Additional studies are required to clarify the origin of this important phenomenon which controls scramjet performance and efficiency. The uncertainty and disagreement of these opinions

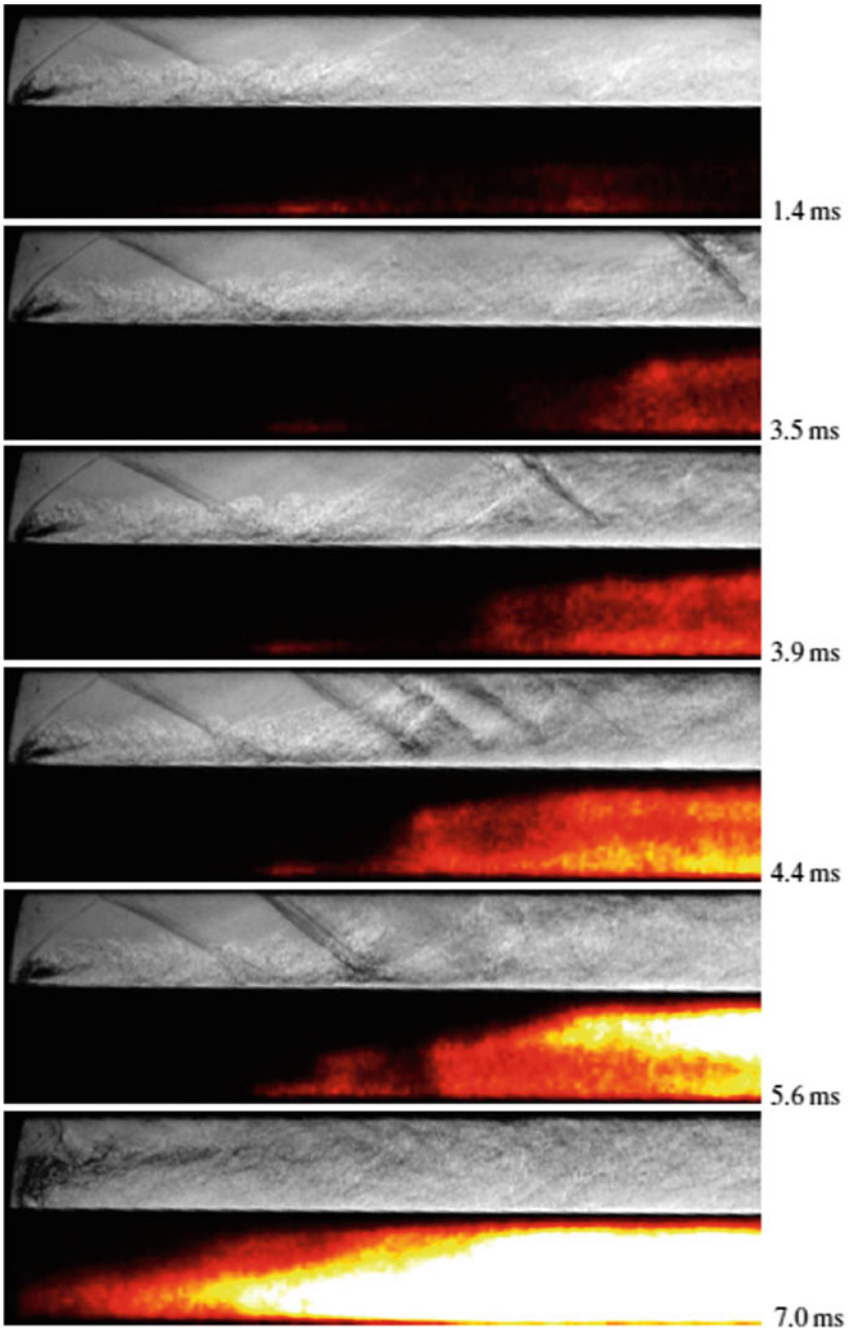

Fig. 1.24 Sequences of quasi-synchronous schlieren and OH* chemiluminescence images of the flow near the injector (x = 56–136 mm) for an equivalence ratio of $\varphi \approx 0.66$ [143]

require continuous and further research on this unsteady process. According to the public literatures, the influence of injection parameters on the combustion oscillation and flashback in a scramjet combustor has barely been researched so far.

1.5 Combustion Near Blowout Limits

The unsteady nature of turbulent combustion has been observed over a wide range of conditions including subsonic flow [56, 153], supersonic flow [131, 135], premixed combustions [154], and non-premixed combustions [155]. While in this section, the unsteady characteristics of combustions near blowout limits in supersonic flows are concerned specially, since it has been observed that the flame unsteadiness in a supersonic flow is remarkably increased when approaching blowout limits [156]. Since the combustion behaviors near lean and rich blowout limits are considerably different from those in moderate combustion, it is necessary to study the blowout limits and the corresponding flame behaviors of supersonic combustion. The existing relevant literatures are selected and summarized below.

1.5.1 Blowout Limits

Blowout limits, including rich blowout limit (RBO) and lean blowout limit (LBO), are the boundaries between stable combustion and flame blowout. Experimentally, the rich or lean blowout limits are respectively defined as the maximum or minimum fuel flow rates or equivalence ratios that are able to sustain continuous combustion. The blowout limits usually depend on the conditions of inflow, fuel types, fuel injection patterns, and the configuration of the cavity [157]. Most of the previous researches concentrated on premixed flames, Ozawa curve [158] gave a parabolic correlation of the blowout limits for a premixed system, which indicated that the flame can only be stabilized within a certain range of conditions thus either excess or insufficiency of any dominant condition can lead to unsteadiness.

For supersonic combustion, the fuel is injected into supersonic air inflow, the combustion process is strongly non-premixed, and thus the process is more complicated than premixed combustion [159]. A number of previous experiments [160–162] have demonstrated that non-premixed lifted jet flame is stabilized on the stoichiometric contour. Although fuel and air are non-premixed at the beginning, the condition at flame base is premixed after the mixing process within the lift distance. Based on the view of non-premixed combustion and combined with experimental data, Driscoll and Rasmussen [163] developed a correlation model to predict the blowout limits of a cavity in supersonic flow. The model avoided the assumption of perfectly stirred reactor (PSR) in premixed flames, and could be applied to cavities, steps, and struts in supersonic flows.

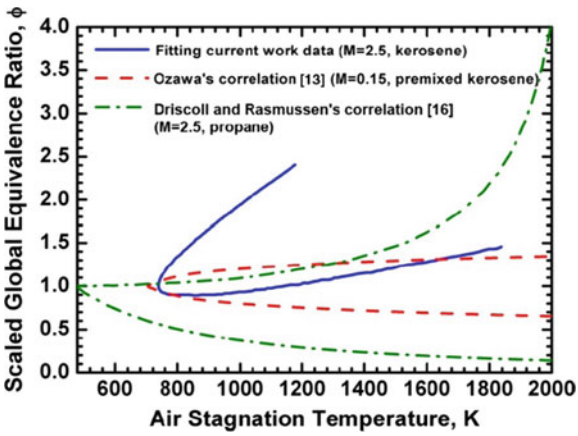

Fig. 1.25 Comparison of three existing correlations [157]

In order to study the effects of different conditions on the blowout limits, Zhang et al. [157] performed several sets of experiments in supersonic combustors. The stagnation temperature of the inflow and the injection pattern were observed to be the dominant parameters, while the impact of air stagnation pressure and the combustor divergence angle were negligible. Figure 1.25 shows the comparison of the three different correlations mentioned above. Experiments performed by Donohue et al. [164] also gave the same pattern of blowout limit correlations.

Retaureau et al. [165] also observed the significant impact of the free stream temperature on the stability domain. In addition, it was reported that the combustion process was barely stable when the static pressure in the combustor was low, thus a certain level of combustor pressure was also crucial in the blowout mechanisms. Different fuel types were also compared, hydrogen was preferred for a wider range of stability domain while ethylene was less sensitive when the static pressure was low.

The mechanism of flame blowout was associated with combustion modes by several researchers. Le et al. [166] divided the combustion stabilization mode into two different types: shear layer stabilization mode and recirculation zone stabilization mode. In the former mode, the flame base was anchored downstream of the cavity leading edge. While in the latter mode, the flame base was attached to the top of the cavity leading edge, and the flame was deep in the cavity, which lifted the shear layer up, expanded the mixing area of fuel and air, and thus more fuel could enter into the cavity. The flame was stabilized in the shear layer when near LBO limit, as the equivalence ratio decreased, less fuel was in the shear layer, and the flame base moved downstream. When the flame base shifted out of the shear layer, blowout occurred. As for RBO cases, the flame was stabilized in the shear layer at the beginning, the spread velocity of the flame at flame base was decided by the temperature of upstream unburnt gas. When fuel flow rate rose up to RBO limit, more cold fuels entered into the recirculation zone, lowering the heat release, the spread velocity then dropped,

which finally made the lift distance increase beyond the length of shear layer and reaches RBO limit.

It can be concluded from the above literatures that the blowout limits are essentially dominated by the temperature and the fuel distribution. When combustion takes place near blowout limits, the change of the local conditions lead to different behaviors of the margin states.

1.5.2 Combustion Behaviors Near Blowout Limits

The combustion behaviors near blowout limits are remarkably different from those in stable states, and have considerable characteristics of unsteadiness. As concluded above, when the flow and reaction conditions approach critical points, some of the parameters intermittently overstep the boundary of stable combustion, which can couple with other sources of oscillations and enhance the degree of unsteadiness. The combustion behaviors near blowout limits, therefore, have drawn some attentions of the researchers.

The distributions of the reaction zones were initially observed to be different between stable states and margin states. Rasmussen et al. [167–169] reported the flame location within the cavity at different fueling rates, and analyzed the qualitative effect of heat release in the cavity on flow oscillations. Figure 1.26 shows the location of reaction zone near LBO and RBO limits. Near LBO, reaction zone moved into cavity volume for both wall injection and floor injection; while wall fueled flame moves to rear of cavity and floor fueled flame extended to length of cavity when RBO is approached.

Lin et al. [170, 171] investigated the flame structures and operating limits of an ethylene-fueled recessed cavity flameholder both experimentally and numerically. Figure 1.27 shows the instantaneous images from a high-speed video camera for cavity flames with various independent cavity fuel flow rates, and near LBO the

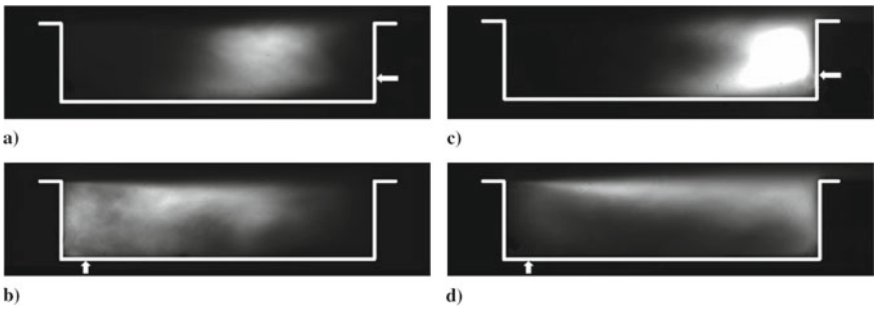

Fig. 1.26 Near lean blowout, reaction zone moves into cavity volume for both **a** wall injection and **b** floor injection; at high fueling rates approaching RBO, wall fueled flame **c** moves to rear of cavity and floor fueled flame **d** extends to length of cavity [168]

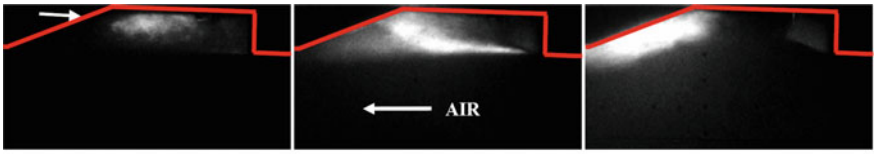

Fig. 1.27 Instantaneous images from a high-speed video camera for cavity flames with various independent cavity fuel flow rates for Mflight = 5.0 and q = 1000 psf. **a** Near lean blowout limit, 0.0011 lb/s, **b** Near rich ignition limit, 0.0047 lb/s, **c** Near rich blowout limit, 0.0089 lb/s [169]

flame was anchored near cavity floor and near RBO the flame moves downstream to cavity trailing edge. The numerical study also discovered the same characteristics near LBO.

The difference in the flame locations is partially due to fuel transport and convection. Choi et al. [172] employed Linear Eddy Mixing (LEM) Model as a subgrid closure for turbulent combustion in Large Eddy Simulation (LES), and numerically investigated stable combustion and blowout limits. The results showed that the fuel (a blended mixture of methane and hydrogen) was mostly found in the injection region. Some methane was convected along the shear layer and mixed with oxygen in the aft region of the cavity, but not enough hydrogen was present. It was observed that in the blowout case the flow structure inside the cavity was substantially different from the stable case.

Further researches indicated that the flow field would also change significantly when approaching blowout limits. According to Ghodke et al. [173], in stable combustion, a large vortical flow was formed in the aft region of the cavity that provided an effective mechanism to transport the hot products and to enhance mixing of the fuel-air mixture. While small localized vortical flow structures were seen in the near-blowout case that did not seem to be as efficient in mixing the hot products and/or in transporting the premixed mixture. Tuttle et al. [174] also observed increased streamwise oscillations in the flow field near rich blowout limit through particle image velocimetry (PIV).

Researches employing high frequency detection techniques further discovered the enhanced unsteady behaviors of combustions near blowout limits. Allen et al. [175] used standard deviation images to characterize the flame unsteadiness, and reported fluctuations of the flame distribution. Gruber et al. [156] reported increased emission fluctuations near lean blowout limit. The frequency spectra showed that the oscillations near lean blowout limit were governed by low frequencies below 250 Hz, and it was mainly caused by the reignition processes.

Hammak et al. [155] employed high-repetition-rate OH PLIF to observe the unsteady phenomena corresponding to the supersonic combustion in a cavity flameholder near lean blowout limit. As shown in Fig. 1.28, the averaged result showed that the flame was mainly stabled close to the aft wall of the cavity, while the sequential images showed that the flame was periodically convected and the combustion was extremely weak.

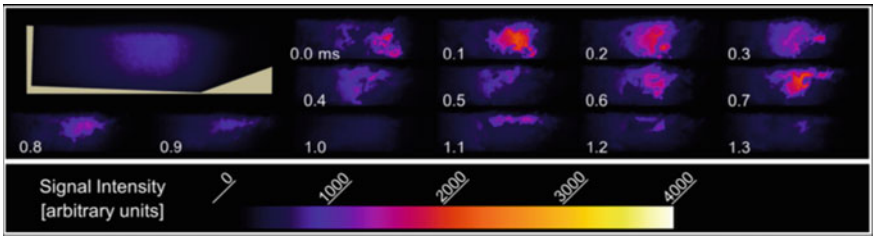

Fig. 1.28 Average and sequential images for lean blowout condition [155]

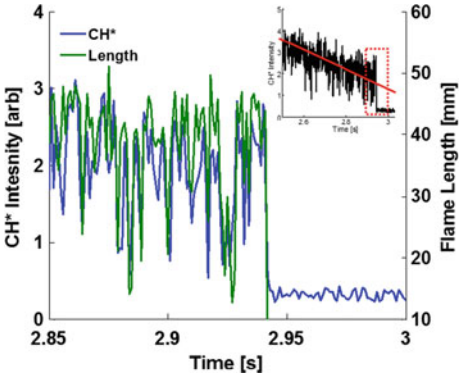

Fig. 1.29 Temporal comparison of integrated CH* signal and flame length in the moments before LBO showing that shortening of the flame is correlated with decreased heat release. The inset image depicts a general downward trend in overall CH* signal as the equivalence ratio is reduced [154]

Allison et al. [154] detected the dynamic characteristics of premixed ethylene flame near LBO by high-speed CH* chemiluminescence. In Fig. 1.29 the integrated CH* signal intensity is compared with the flame length, which reveals that the strong oscillations of the flame near LBO are correlated with the heat release.

1.5.3 Summary

Blowout limits are the boundaries between stable combustion and flame blowout, including rich blowout limit and lean blowout limit. The combustion behaviors near blowout limits are distinctly different from stable combustion, the flame unsteadiness in a supersonic flow is remarkably increased when approaching blowout limits. Supersonic combustion is strongly non-premixed, and the process is more complicated than premixed combustion. The change of the local conditions lead to different behaviors of the margin states. The existing literatures observed the unsteady characteristics near blowout limits, and quantitative analyses indicated that the unsteady nature could be associated with the flow field oscillations, the reignition process, and the heat release fluctuations in the margin state.

The behavior of the flame that is actually experiencing the blowout process is still observed in recent studies, which provide more information in characterizing the unsteady behaviors of combustion near blowout limits. In order to describe the unsteady behavior near blowout limits, it is necessary to further study the flame mechanism near blowout limits.

1.6 Discussion

A review of unsteady combustion physics in supersonic flows has been presented, trying to construct a framework for unsteady supersonic combustion and provide a guideline for future study. The topics cover several fundamental aspects, including interactions between acoustic wave and flame, Flow Dominating Instability, ignition, flame flashback and near-blowout combustion. The conclusions are drawn as below.

It is a common assumption that acoustic waves cannot travel upstream in a supersonic flow, and any flow oscillations arising in the flame zone will simply travel downstream and exit from the engine without forming the feedback loop required to sustaining combustion and flow instabilities. However, the researches indicates that there are various subsonic flow regions in scramjets. Acoustic wave induced by perturbations can propagate upstream in subsonic regions embedded in supersonic flows. Interactions among flame, shock wave and fuel injection may give rise to acoustic feedback loops, and pay a contribution to the sustainability of unsteadiness in supersonic reacting flows. Interactions of combustion and acoustic wave in scramjet combustors still need to be further explored so that the thermoacoustic effects may be controlled efficiently. In this work, the researches about the combustion oscillation characteristics in the scramjet combustor will be introduced, which are shown in Chap. 2.

The flow dominating instability is believed to occur when separation is severe, and is usually accompanied by asymmetric flow field structures. The frequency feature of unsteady separated flow is broadband, and major frequency components of oscillation concentrate in low frequency. Interactions between separated shocks and shear layer instabilities may be account for a certain type of unsteadiness. Due to the intrinsic complexities in shock wave-boundary layer interactions, the mechanism of unsteady combustion induced by backpressure forced separation remains unclear. Further studies are required to study the unsteadiness of separation in reacting flows. Chapter 3 focuses on the study of combustion unsteadiness dominated by shock-induced separation. For a rectangular supersonic combustor with dual parallel cavities and near-cavity fuel injections, flowfield structures generally transform from symmetry into asymmetry as the increment of equivalence ratio. Under an intermediate equivalence ratio, intermittent dynamic combustion occurs with a high-amplitude pseudo-shock oscillation in the streamwise direction. A decoupling analysis is carried out to discover the key impact factor of this unsteady combustion, it is found that the flame, fuel jet as well as cavity flameholder do not play a key role in this issue. Thus, cold flow analysis is applied, and the typical flame structures are fully reproduced

by the backpressure induced separated flowfield. Specifically speaking, a symmetric separation under low backpressure generates symmetric combustion, while an asymmetric separation under high backpressure results in asymmetric combustion. Based on the detached-eddy simulation, the whole process of symmetric/asymmetric separation transition (occurs under threshold backpressure) is captured. Boundary layer separation tendency analysis shows that an interlaced shape factor distribution of the boundary layers from both walls accounts for the switch of separation modes.

Although significant research progress regarding cavity ignition in a supersonic flow has been achieved in the recent years, the understanding of the cavity ignition mechanism is still far from being satisfactory. The effects of auto-ignition on combustion stabilization have also been analyzed preliminary, and qualitative results have been obtained. The recent research of our work on the characteristics of the ignition process in the cavity-based supersonic combustion will be introduced in Chap. 4 typical ignition processes under diverse ignition methods will be presented, involving the spark ignition, the piloted ignition, the gliding-arc-discharge ignition and LIP ignition. This section aims to first introduce general ignition methods with their features, and second provide an intuitive observation on the dynamic ignition process. Tthe flame behaviors during ignition is emphasized from two aspects, namely flame kernel formation and initial flame propagation. The studies of flame kernel formation and flame propagation are conducted in single-cavity combustors, showing the effects of ignition energy, ignition position and rear wall height. The analysis of the ignition mechanism is introduced and the effects of the auto-ignition in the combustor with transverse injection is primarily explained.

Due to relatively long premixing length, a lean premixed gas mixture often induces the combustion oscillation in scramjet engines, which can directly degrade the engine performance and reduce its life cycle. Hence, it is important to explore the mechanism of the flame flashback, and devise possible control methods. Chapter 5 would show the experimental results and discusses the factors inducing combustion oscillation, such as the global equivalence-ratio, the pre-mixing distance, the injection angle, and the jets number. A simplified combustion opening system model will be constructed for mechanism analysis.

Studying the mechanism of blowout limits is of great value for understanding the unsteady characteristics of turbulent combustion and the flame behaviour near blowout. The existing literatures observed the unsteady characteristics near blowout limits, and quantitative analyses indicated that the unsteady nature could be associated with the flow field oscillations, the re-ignition process, and the heat release fluctuations in the margin state. In Chap. 6, blowout limits of cavity flame in supersonic flows is firstly analysed and modelled. Then, mixing and combustion characteristics with different injection schemes in low equivalence ratio conditions are investigated experimentally and numerically. At last, the flame blowout and re-ignition of premixed flame and non-premixed flame are studied systematically.

References

1. Curran, E. T. (2001). Scramjet engines: The first forty years. *Journal of Propulsion and Power, 17,* 1138–1148.
2. Rayleigh, J. (1878). The explanation of certain acoustical phenomena. *Nature, 18*(455), 319–321.
3. Ducruix, S., Schuller, T., Durox, D., & Candel, S. (2003). Combustion dynamics and instabilities: Elementary coupling and driving mechanisms. *Journal of Propulsion and Power*, *19*, 722–734.
4. Balachandran, R., Ayoola, B. O., Kaminski, C. F., Dowling, A. P., & Mastorakos, E. (2005). Experimental investigation of the nonlinear response of turbulent premixed flames to imposed inlet velocity oscillations. *Combustion and Flame, 143,* 37–55.
5. Hardi, J., Oschwald, M., & Dally, B. (2011). Flame response to acoustic excitation in a rectangular rocket combustor with LO_x/H_2 propellants. *Ceas Space Journal, 2,* 41–49.
6. Stamp, G., Ghosh, A., Zang, A., & Yu, K. (2005). Experimental characterization of acoustic wave propagation in a supersonic duct. In *41st AIAA/ASME/SAE/ASEE Joint Propulsion Conference & Exhibit* (p. 4144). AIAA.
7. Wang, H., Sun, M., Qin, N., Wu, H., & Wang, Z. (2013). Characteristics of oscillations in supersonic open cavity flows. *Flow, Turbulence and Combustion, 90,* 121–142.
8. Lin, K.-C., & Jackson, K. (2007). Acoustic characterization of an ethylene-fueled scramjet combustor with a recessed cavity flameholder. In *43rd AIAA/ASME/SAE/ASEE Joint Propulsion Conference & Exhibit* (p. 5382). AIAA.
9. Choi, J.-Y., Ma, F., & Yang, V. (2005). Dynamic combustion characteristics in scramjet combustors with transverse fuel injection. In *41st AIAA/ASME/SAE/ASEE Joint Propulsion Conference & Exhibit* (p. 4428). AIAA.
10. Choi, J.-Y., Ma, F., Yang, V., Won, S.-H., & Jeung, I.-S. (2007). Detached eddy simulation of combustion dynamics in scramjet combustors. In *43rd AIAA/ASME/SAE/ASEE Joint Propulsion Conference & Exhibit* (p. 5027). AIAA.
11. Ma, F., Li, J., Yang, V., Lin, K., & Jackson, T. (2005). Thermoacoustic flow instability in a scramjet combustor. In *41st AIAA/ASME/SAE/ASEE Joint Propulsion Conference & Exhibit* (p. 3824). AIAA.
12. Li, J., Ma, F., Yang, V., Lin, K.-C., & Jackson, T. (2007). A comprehensive study of combustion oscillations in a hydrocarbon-fueled scramjet engine. In *45th AIAA Aerospace Sciences Meeting and Exhibit* (p. 836). AIAA.
13. Lin, K. C., Jackson, K., Behdadnia, R., Jackson, T. A.,Ma, F. H., & Yang, V. (2010). Acoustic characterization of an ethylene-fueled scramjet combustor with a cavity flameholder. *Journal of Propulsion and Power, 26*, 1161–1170.
14. Frost, M. A., Gangurde, D. Y., Paull, A., & Mee, D. J. (2009). Boundary-layer separation due to combustion-induced pressure rise in a supersonic flow. *AIAA Journal, 47,* 1050–1053.
15. Knight, D., Yan, H., Panaras, A. G., & Zheltovodov, A. (2003). Advances in CFD prediction of shock wave turbulent boundary layer interactions. *Progress in Aerospace Sciences, 39,* 121–184.
16. Dolling, D. S. (2001). Fifty years of shock-wave/boundary-layer interaction research: What next? *AIAA Journal, 39,* 1517–1531.
17. Dolling, D. S., & Erengil, M. E. (1991). Unsteady wave structure near separation in a Mach 5 compression rampinteraction. *AIAA Journal, 29,* 728–735.
18. Schmisseur, J. D., & Dolling, D. S. (1994). Fluctuating wall pressures near separation in highly swept turbulent interactions. *AIAA Journal, 32,* 1151–1157.
19. Erengil, M. E., & Dolling, D. S. (1993). Effects of sweepback on unsteady separation in Mach 5 compression ramp interactions. *AIAA Journal, 31,* 302–311.
20. Brusniak, L., & Dolling, D. S. (1994). Physics of unsteady blunt-fin-induced shock wave/turbulent boundary layer interactions. *Journal of Fluid Mechanics, 273,* 375–409.
21. Dolling, D. S., & Brusniak, L. (1989). Separation shock motion in fin, cylinder, and compression ramp—Induced turbulent interactions. *AIAA Journal, 27,* 734–742.

22. Dupont, P., Haddad, C., & Debiève, J. F. (2006). Space and time organization in a shock-induced separated boundary layer. *Journal of Fluid Mechanics, 559,* 255–277.
23. Clemens, N. T., & Narayanaswamy, V. (2014). Low-frequency unsteadiness of shock wave/turbulent boundary layer interactions. *Annual Review of Fluid Mechanics, 46,* 469–492.
24. Dolling, D. S., & Murphy, M. T. (1983). Unsteadiness of the separation shock wave structure in a supersonic compression ramp flowfield. *AIAA Journal, 21,* 1628–1634.
25. Humble, R. A., Elsinga, G. E., Scarano, F., & Oudheusden, B. W. V. (2009). Three-dimensional instantaneous structure of a shock wave/turbulent boundary layer interaction. *Journal of Fluid Mechanics, 622,* 33–62.
26. Priebe, S., & Martín, M. P. (2012). Low-frequency unsteadiness in shock wave-turbulent boundary layer interaction. *Journal of Fluid Mechanics, 699,* 1–49.
27. Pasquariello, V., Hickel, S., & Adams, N. A. (2017). Unsteady effects of strong shock-wave/boundary-layer interaction at high Reynolds number. *Journal of Fluid Mechanics, 823,* 617–657.
28. Piponniau, S., Dussauge, J. P., Debiève, J. F., & Dupont, P. (2009). A simple model for low-frequency unsteadiness in shock-induced separation. *Journal of Fluid Mechanics, 629,* 87–108.
29. Koo, H., & Raman, V. (2012). Large-eddy simulation of a supersonic inlet-isolator. *AIAA Journal, 50,* 1596–1613.
30. Do, H., Im, S. K., Mungal, M. G., & Cappelli, M. A. (2011). The influence of boundary layers on supersonic inlet flow unstart induced by mass injection. *Experiments in Fluids, 51,* 679–691.
31. Zhang, Q. F., Tan, H. J., Sun, S., Bu, H. X., & Rao, C. Y. (2016). Unstart of a hypersonic inlet with side compression caused by downstream choking. *AIAA Journal, 54*(1), 28–38.
32. Jonathan, G., & Kenneth, Y. (2012). Experimental characterization of isolator shock train propagation. In *18th AIAA/3AF International Space Planes and Hypersonic Systems and Technologies Conference* (p. 5891). AIAA.
33. Jonathan, S. G., & Kenneth, H. Y. (2013). Visualization of shock train-boundary layer interaction in Mach 2.5 isolator flow. In *43rd Fluid Dynamics Conference* (p. 3102). AIAA.
34. Bruce, P. J. K., Babinsky, H., Tartinville, B., & Hirsch, C. (2011). Corner effect and asymmetry in transonic channel flows. *AIAA Journal, 49,* 2382–2392.
35. Su, W.-Y., & Zhang, K.-Y. (2012). Back-pressure effects on the hypersonic inlet-isolator pseudoshock motions. *Journal of Propulsion and Power, 29,* 1391–1399.
36. Su, W.-Y., Ji, Y.-X., & Chen, Y. (2016). Effects of dynamic backpressure on pseudoshock oscillations in scramjet inlet-isolator. *Journal of Propulsion and Power, 32,* 516–528.
37. Li, N., Chang, J.-T., Xu, K.-J., Yu, D.-R., Bao, W., & Song, Y.-P. (2018). Oscillation of the shock train in an isolator with incident shocks. *Physics of Fluids, 30,* 116102.
38. Xiong, B., Wang, Z. G., Fan, X. Q., & Wang, Y. (2017). Response of shock train to high-frequency fluctuating backpressure in an isolator. *Journal of Propulsion and Power, 33,* 1–9.
39. Xiong, B., Fan, X.-Q., Wang, Z.-G., & Tao, Y. (2018). Analysis and modelling of unsteady shock train motions. *Journal of Fluid Mechanics, 846,* 240–262.
40. Reijasse, P., Corbel, B., & Soulevant, D. (1999). Unsteadiness and asymmetry of shock-induced separation in a planar two-dimensional nozzle—A flow description. In *30th Fluid Dynamics Conference* (p. 3694). AIAA.
41. Yu, Y., Xu, J., Mo, J., & Wang, M. (2014). Principal parameters in flow separation patterns of over-expanded single expansion RAMP nozzle. *Engineering Applications of Computational Fluid Mechanics, 8,* 274–288.
42. Yu, Y., Xu, J., Yu, K., & Mo, J. (2015). Unsteady transitions of separation patterns in single expansion ramp nozzle. *Shock Waves, 25,* 623–633.
43. Dimitri, P., & Andreas, Z. (2004). Fundamental investigation of supersonic nozzle flow separation. In *42nd AIAA Aerospace Sciences Meeting and Exhibit* (p. 1111). AIAA.
44. Dimitri, P., & Andrew, J. (2006). Unsteady phenomena in supersonic nozzle flow separation. In *36th AIAA Fluid Dynamics Conference and Exhibit* (p. 3360). AIAA.

45. Xiao, Q., Tsai, H.-M., & Papamoschou, D. (2007). Numerical investigation of supersonic nozzle flow separation. *AIAA Journal, 45,* 532–541.
46. Johnson, A. D., & Papamoschou, D. (2010). Instability of shock-induced nozzle flow separation. *Physics of Fluids*, *22*, 016102.
47. Olson, B., & Lele, S. (2012). Low frequency unsteadiness in nozzle flow separation. In *42nd AIAA Fluid Dynamics Conference and Exhibit* (p. 2974). AIAA.
48. Olson, B., & Lele, S. (2011). Large-eddy simulation of an over-expanded planar nozzle. In *41st AIAA Fluid Dynamics Conference and Exhibit* (p. 3908). AIAA.
49. Andrew, J., & Dimitri, P. (2008). Shock motion and flow instabilities in supersonic nozzle flow separation. In *38th Fluid Dynamics Conference and Exhibit* (p. 1111). AIAA.
50. Papamoschou, D., Zill, A., & Johnson, A. (2009). Supersonic flow separation in planar nozzles. *Shock Waves, 19,* 171–183.
51. Laurence, S. J., Lieber, D., Martinez Schramm, J., Hannemann, K., & Larsson, J. (2015). Incipient thermal choking and stable shock-train formation in the heat-release region of a scramjet combustor. Part I: Shock-tunnel experiments. *Combustion and Flame*, *162*, 921–931.
52. Fotia, M. L., & Driscoll, J. F. (2013). Ram-scram transition and flame/shock-train interactions in a model scramjet experiment. *Journal of Propulsion and Power, 29,* 261–273.
53. Yuan, Y., Zhang, T., Yao, W., & Fan, X. (2015). Study on flame stabilization in a dual-mode combustor using optical measurements. *Journal of Propulsion and Power, 31,* 1524–1531.
54. Zhao, D., Gutmark, E., & de Goey, P. (2018). A review of cavity-based trapped vortex, ultra-compact, high-g, inter-turbine combustors. *Progress in Energy and Combustion Science, 66,* 42–82.
55. Huang, Y., & Yang, V. (2009). Dynamics and stability of lean-premixed swirl-stabilized combustion. *Progress in Energy and Combustion Science, 35,* 293–364.
56. Santosh, S., Sajjad, H., & Tim, L. (2009). Lean blowoff of bluff body stabilized flames—Scaling and dynamics. *Progress in Energy and Combustion Science, 35,* 98–120.
57. Penner, S. S., & Williams, F. (1957). Recent studies on flame stabilization of premixed turbulent gases. *Applied Mechanics Review*, *10*.
58. Schadow, K. C., & Gutmark, E. (1992). Combustion instability related to vortex shedding in dump combustors and their passive control. *Progress in Energy and Combustion Science*, *18*, 117–132.
59. Lefebvre, A. H.,& Whitelaw, J. H. (1984). Gas turbine combustion. *International Journal of Heat and Fluid Flow*, *5*(4), 228.
60. Lee, J. G., Armstrong, J. P., & Santavicca, D. A. (2011). Experimental on lean blowout and Nox emissions of a premixed trapped vortex combustor with high G-loading. *Proceedings of ASME Turbo Expo 2011, GT2011-46396*. British Columbia, Canada: Vancouver.
61. Xing, F., Wang, P., Zhang, S., Zou, J., Zheng, Y., & Zhang, R., et al. (2012). Experiment and simulation study on lean blow-out of trapped vortex combustor with various aspect ratios. *Aerospace Science and Technology, 18,* 48–55.
62. Xing, F., Fan, W., & Yang, M. (2009). Experiments and simulation study on flow field and LBO of trapped vortex combustor with H/L changed. In *45th AIAA/ASME/SAE/ASEE Joint Propulsion Conference and Exhibit*.
63. Biagioli, F., Güthe, F., & Schuermans, B. (2008). Combustion dynamics linked to flame behaviour in a partially premixed swirled industrial burner. *Experimental Thermal and Fluid Science, 32,* 1344–1353.
64. McManus, K. R., Poinsot, T., & Candel, S. M. (1993). A review of active control of combustion instabilities. *Progress in Energy and Combustion Science, 19,* 1–29.
65. Ben-Yakar, A., & Hanson, R. K. (2001). Cavity flame-holders for ignition and flame stabilization in scramjets: An overview. *Journal of Propulsion and Power, 17*(4), 869–878.
66. Sturgess, G. J., Zelina, J., Shouse, D. T., & Roquemore, W. M. (2005). Emissions reduction technologies for military gas turbine engines. *Journal of Propulsion and Power, 21,* 193–217.
67. Hsu, K., Gross, L., Trump, D., Roquemore, W. (1995). Performance of a trapped-vortex combustor. In *33rd Aerospace Sciences Meeting and Exhibit* (p. 810). AIAA.

68. Mongia, H., Gore, J., Grinstein, F., Gutmark, E., Jeng, S. M., McDonell, V., Menon, S., Samuelsen, G., Santavicca, D., & Santoro, R. (2001). Combustion research needs for helping development of next-generation advanced combustors. In *37th Joint Propulsion Conference and Exhibit* (p. 3853). AIAA.
69. Shouse, D. T. (2000). *Trapped vortex combustion technology MITE workshop*. Dayton Ohio, USA: US Air Force Research Laboratory, Wright-Patterson Air Force Base.
70. Gruber, M. R., Baurle, R. A., Mathur, T., & Hsu, K. Y. (2001). Fundamental studies of cavity-based flameholder concepts for supersonic combustors. *Journal of Propulsion and Power, 17,* 146–153.
71. Yu, K. H., Wilson, K. J., & Schadow, K. C. (2001). Effect of flame-holding cavities on supersonic-combustion performance. *Journal of Propulsion and Power, 17,* 1287–1295.
72. Ben-Yakar, A., Hanson, R. K. (1998). *Cavity flame-holders for ignition and flame stabilization in scramjets: Review and experimental study*. In *34th AIAA/ASME/SAE/ASEE Joint Propulsion Conference and Exhibit* (p. 3122). AIAA.
73. Chen, S. (2016). *Numerical study of trapped vortex combustors characteristics in small Ramjets*. Singapore: Nanyang Technological University.
74. Ballal, D. R., & Lefebvre, A. H. (1977). Ignition and flame quenching in flowing gaseous mixtures. *Proceedings of the Royal Society A, 357,* 163–181.
75. Ballal, D. R., & Lefebvre, A. H. (1978). Ignition and flame quenching of quiescent fuel mists. *Proceedings of the Royal Society A, 364,* 277–294.
76. Ballal, D. R., & Lefebvre, A. H. (1981). A general model of spark ignition for gaseous and liquid fuel-air mixtures. *Symposium (International) on Combustion, 18*(1), 1737–1746.
77. Mastorakos, E. (2009). Ignition of turbulent non-premixed flame. *Progress in Energy and Combustion Science, 35,* 57–97.
78. Zhao, Y., Liang, J., Zhao, Y., & Duan, J. (2017). Research on interactions between cavity and upstream transverse jet in supersonic combustor. In *21st AIAA International Space Planes and Hypersonics Technologies Conference, AIAA 2017–2368*.
79. Li, J., Zhang, L., Choi, J. Y., Yang, V., & Lin, K.-C. (2014). Ignition transients in a scramjet engine with air throttling part 1: Nonreacting flow. *Journal of Propulsion and Power, 30*, 438–448.
80. McNeill, D.H. (2005). Minimum ignition energy for laser spark ignition. *Proceedings of the Combustion Institute, 30*(2), 2913–2920.
81. Brieschenk, S., O'Byrne, S., & Kleine, H. (2013). Laser-induced plasma ignition studies in a model scramjet engine. *Combustion and Flame, 160*, 145–148.
82. Brieschenk, S., O'Byrne, S., & Kleine, H. (2014). Ignition characteristics of laser-ionized fuel injected into a hypersonic crossflow. *Combustion and Flame, 161*, 1015–1025.
83. Denman, Z. J., Chan, W. Y. K., Brieschenk, S., Veeraragavan, A., Wheatley, V., & Smart, M. K. (2016). Ignition experiments of hydrocarbons in a Mach 8 shape-transitioning scramjet engine. *Journal of Propulsion and Power, 32*(6), 1462–1471.
84. Ombrello, T., Peltier, S., & Carter, C. (2015). Effects of inlet distortion on cavity ignition in supersonic flow. In *53rd AIAA Aerospace Sciences Meeting* (p. 0882). AIAA.
85. Ombrello, T., Carter, C., Tam, C.-J., & Hsu, K.-Y. (2014). Cavity ignition in supersonic flow by pulse detonation. In *AIAA SciTech Forum 52nd Aerospace Sciences Meeting* (p. 0286). AIAA.
86. Ombrello, T., Carter, C., McCall, J., & Schauer, F. (2015). Enhanced mixing in supersonic flow using a pulse detonator. *Journal of Propulsion and Power, 31,* 654–663.
87. Miller, J. D., Peltier, S. J., Slipchenko, M. N., Mance, J. G., Ombrello, T. M., & Gord, J. R., et al. (2017). Investigation of transient ignition processes in a model scramjet pilot cavity using simultaneous 100 kHz formaldehyde planar laser-induced fluorescence and CH* chemiluminescence imaging. *Proceedings of the Combustion Institute, 36,* 2865–2872.
88. Cuppoletti, D., Ombrello, T., & Rein, K. (2019). Energy coupling mechanism for pulse detonation ignition of a scramjet cavity. *Proceedings of the Combustion Institute, 37,* 3453–3460.

89. Li, J., Zhang, L., Choi, J. Y., Yang, V., & Lin, K.-C. (2015). Ignition transients in a scramjet engine with air throttling part II: Reacting flow. *Journal of Propulsion and Power, 31,* 79–88.
90. An, B., Wang, Z., Yang, L., Li, X., & Zhu, J. (2017). Experimental investigation on the impacts of ignition energy and position on ignition processes in supersonic flows by laser induced plasma. *Acta Astronautica, 137,* 444–449.
91. Yang, L., Li, X., Liang, J., Yu, Y., Yu, X. (2015). Laser-induced plasma ignition of hydrocarbon fuel in supersonic flows. In *20th AIAA International Space Planes and Hypersonic Systems and Technologies Conference* (p. 3544). AIAA.
92. Yang, L., An, B., Liang, J., Li, X., & Wang, Z. (2018). Dual-pulse laser ignition of ethylene-air mixtures in a supersonic combustor. *Optics Express, 26,* 7911–7919.
93. An, B., Wang, Z., Yang, L., Li, X., & Liu, C. (2019). The ignition characteristics of the close dual-point laser ignition in a cavity based scramjet combustor. *Experimental Thermal and Fluid Science, 101,* 136–140.
94. Li, X., Liu, W., Pan, Y., Yang, L., & An, B. (2017). Experimental investigation on laser-induced plasma ignition of hydrocarbon fuel in scramjet engine at takeover flight conditions. *Acta Astronautica, 138,* 79–84.
95. Li, X., Liu, W., Pan, Y., Yang, L., An, B., & Zhu, J. (2018). Characterization of ignition transient processes in kerosene-fueled model scramjet engine by dual-pulse laser-induced plasma. *Acta Astronautica, 144,* 23–29.
96. Tropina, A. A., Miles, R. B., & Shneider, M. N. (2018). Mathematical model of dual-pulse laser ignition. *Journal of Propulsion and Power, 34,* 408–414.
97. Gibbons, N., Gehre, R., Brieschenk, S., & Wheatley, V. (2018). Simulation of laser-induced plasma ignition in a hypersonic crossflow. *AIAA Journal, 56*(8), 3047–3059.
98. Firsov, A. A., Shurupov, M. A., Yarantsev, D. A.,& Leonov, S. B. (2014). Plasma-assisted combustion in supersonic airflow: Optimization of electrical discharge geometry. In *52nd Aerospace Sciences Meeting*. AIAA.
99. Leonov, S. B., Firsov, A. A., Yarantsev, D. A., Falempin, F.,& Miller, A. (2009). Flow control in model supersonic inlet by electrical discharge. In *16th AIAA/DLR/DGLR International Space Planes and Hypersonic Systems and Technologies Conference* (p. 7367). AIAA.
100. Firsov, A. A., Dolgov, E. V., Rakhimov, R. G., Shurupov, M. A., & Leonov, S. B. (2018). Mixing enhancement by electrical discharge in supersonic airflow. In *2018 AIAA Aerospace Sciences Meeting*. AIAA 2018-1195.
101. Savelkin, K. V., Yarantsev, D. A., Adamovichb, I. V., & Leonov, S. B. (2015). Ignition and flameholding in a supersonic combustor by an electrical discharge combined with a fuel injector. *Combustion and Flame, 162,* 825–835.
102. Leonov, S., Houpt, A., Elliott, S., & Hedlund, B. (2018). Ethylene ignition and flameholding by electrical discharge in supersonic combustor. *Journal of Propulsion and Power, 34,* 499–509.
103. Feng, R., Li, J., Wu, Y., Zhu, J., Song, X., & Li, X. (2018). Experimental investigation on gliding arc discharge plasma ignition and flame stabilization in scramjet combustor. *Aerospace Science and Technology, 79,* 145–153.
104. Huang, S., Wu, Y., Song, H., Zhu, J., Zhang, Z., Song, X., et al. (2018). Experimental investigation of multichannel plasma igniter in a supersonic model combustor. *Experimental Thermal and Fluid Science, 99,* 315–323.
105. Li, J., Ma, F., Yang, V., Lin, K.-C., & Jackson, T. A. (2007). A comprehensive study of ignition transient in an ethylene-fueled scramjet combustor. In *43rd AIAA/ASME/SAE/ASEE Joint Propulsion Conference & Exhibit* (p. 5025). AIAA.
106. Yang, V., Li, J., Choi, J. Y., & Lin, K.-C. (2010). Ignition Transient in an Ethylene Fueled Scramjet Engine with Air Throttling Part II: Ignition and Flame Development. In *48th AIAA Aerospace Sciences Meeting Including the New Horizons Forum and Aerospace Exposition* (p. 410). AIAA.
107. Li, J., Ma, F., Yang, V., Lin, K.-C., & Jackson, T. A. (2006). Control and optimization of ignition transient in scramjet engine using air throttling. In *44th AIAA Aerospace Sciences Meeting and Exhibit* (p. 1028). AIAA.

108. Noh, J., Choi, J.-Y., Byun, J.-R., Lim, J.-S., & Yang, V. (2010). Numerical simulation of auto-ignition of ethylene in a scramjet combustor with air throttling. In *46th AIAA/ASME/SAE/ASEE Joint Propulsion Conference & Exhibit* (p. 7036). AIAA.
109. Yang, S., Tian, Y., & Le, J. (2017). Flow oscillation in a scramjet combustor with air-throttling. In *21st AIAA International Space Planes and Hypersonics Technologies Conference* (p. 2301). AIAA.
110. Tian, Y., Xiao, B., Zhang, S., & Xing, J. (2015). Experimental and computational study on combustion performance of a kerosene fueled dual-mode scramjet engine. *Aerospace Science and Technology, 46,* 451–458.
111. Tian, Y., Yang, S., & Le, J. (2016). Numerical study on effect of air throttling on combustion mode formation and transition in a dual-mode scramjet combustor. *Aerospace Science and Technology, 52,* 173–180.
112. Tian, Y., Yang, S., Le, J., Zhong, F., & Tian, X. (2017). Investigation of combustion process of a kerosene fueled combustor with air throttling. *Combustion and Flame, 179,* 74–85.
113. Sun, M. B., Gong, C., Zhang, S. P., Liang, J. H., Liu, W. D., & Wang, Z. G. (2012). Spark ignition process in a scramjet combustor fueled by hydrogen and equipped with multi-cavities at Mach 4 flight condition. *Experimental Thermal and Fluid Science, 43,* 90–96.
114. Kim, C.-H., Jeung, I.-S., Choi, B., Kouchi, T., Takita, K., & Masuya, G. (2011). Effect of fuel injection location on a plasma jet assisted combustion with a backward-facing step. *Proceedings of the Combustion Institute, 33,* 2375–2382.
115. Matsubara, Y., Takita, K., & Masuya, G. (2013). Combustion enhancement in a supersonic flow by simultaneous operation of DBD and plasma jet. *Proceedings of the Combustion Institute, 34,* 3287–3294.
116. Matsubara, Y., & Takita, K. (2011). Effect of mixing ratio of N_2/O_2 feedstock on ignition by plasma jet torch. *Proceedings of the Combustion Institute, 33,* 3203–3209.
117. Xi, W., Wang, Z., Sun, M., Liu, W., & Li, Q. (2014). Experimental investigation of ignition transient phase in model supersonic combustor. *Journal of Aerospace Engineering, 27,* 04014009.
118. Situ, M., Wang, C., Lu, H. P., Yu, G., & Zhang, X. Y. (2001). Hot gas piloted energy for supersonic combustion of kerosene with dual-cavity. In *39th AIAA Aerospace Sciences Meeting & Exhibit* (p. 0523). AIAA.
119. Situ, M., Wang, C., & Zhuang, K. (2002). Investigation of supersonic combustion of kerosene jets with hot gas piloted energy and dual-cavity. In *40th AIAA Aerospace Sciences Meeting & Exhibit* (p. 13938). AIAA.
120. Qing, L., Wenxiong, X., Lin, L., Yu, P., Meng, D., & Jianhan, L. (2012). Research on hot gas jet ignition process of scramjet combustor fueled with kerosene. In *18th AIAA/3AF International Space Planes and Hypersonic Systems and Technologies Conference* (p. 5947). AIAA.
121. Sung, C. J., Li, J. G., Yu, G., & Law, C. K. (1999). Chemical kinetics and self-ignition in a model supersonic hydrogen-air combustor. *AIAA Journal, 37,* 208–214.
122. Fureby, C., Nordin-Bates, K., Petterson, K., Bresson, A., & Sabelnikov, V. (2015). A computational study of supersonic combustion in strut injector and hypermixer flow fields. *Proceedings of Combustion Institute*, *35*, 2127–2135.
123. Gordon, R. L., Masri, A. R., & Mastorakos, E. (2008). Simultaneous rayleigh temperature, OH- and CH_2O-LIF imaging of methane jets in a vitiated coflow. *Combustion and Flame, 155,* 181–195.
124. Cabra, R., Chen, J. Y., Dibble, R. W., Karpetis, A. N., & Barlow, R. S. (2005). Lifted methane-air jet flames in a vitiated coflow. *Combustion and Flame, 143,* 491–506.
125. Domingo, P., Vervisch, L., & Veynante, D. (2008). Large-eddy simulation of a lifted methane jet flame in a vitiated coflow. *Combustion and Flame, 152,* 415–432.
126. Domingo, P., Vervisch, L., & Veynante, D. (2006). Auto-ignition and flame propagation effects in LES of burned gases diluted turbulent combustion. *Proceedings of the Summer* Program 2006, 337-348.
127. Yoo, C. S., Richardson, E. S., Sankaran, R., & Chen, J. H. (2011). A DNS study on the stabilization mechanism of a turbulent lifted ethylene jet flame in highly-heated coflow. *Proceedings of the Combustion Institute, 33*(1), 1619–1627.

128. Lu, S., Fan, J., & Luo, K. (2012). High-fidelity resolution of the characteristic structures of a supersonic hydrogen jet flame with heated co-flow air. *International Journal of Hydrogen Energy, 37,* 3528–3539.
129. Micka, D. J., & Driscoll, J. F. (2012). Stratified jet flames in a heated (1390 K) air cross-flow with autoignition. *Combustion and Flame, 159,* 1205–1214.
130. Micka, D. J., & Driscoll, J. F. (2011). Stratified jet flames in a heated (1364 K) cross-flow with auto-ignition. In *49th AIAA Aerospace Sciences Meeting including the New Horizons Forum and Aerospace Exposition* (P. 321). AIAA.
131. Wang, H., Wang, Z., Sun, M., & Qin, N. (2013). Combustion characteristics in a supersonic combustor with hydrogen injection upstream of cavity flameholder. *Proceedings of the Combustion Institute, 34,* 2073–2082.
132. Sun, M. B., Cui, X. D., Wang, H. B., & Bychkov, V. (2015). Flame flashback in a supersonic combustor fueled by ethylene with cavity flameholder. *Journal of Propulsion and Power, 31,* 976–981.
133. Huang, Z. W., He, G. Q., Qin, F., Xue, R., Wei, X. G., & Shi, L. (2016). Combustion oscillation study in a kerosene fueled rocket-based combinedcycle engine combustor. *Acta Astronautica, 129,* 260–270.
134. Wang, Z. G., Sun, M. B., Wang, H. B., Yu, J. F., Liang, J. H., & Zhuang, F. C. (2015). Mixing-related low frequency oscillation of combustion in an ethylene-fueled supersonic combustor. *Proceedings of the Combustion Institute, 35,* 2137–2144.
135. Wang, H., Wang, Z., Sun, M., & Qin, N. (2013). Large-Eddy/Reynolds-averaged Navier-stokes simulation of combustion oscillations in a cavity-based supersonic combustor. *International Journal of Hydrogen Energy, 38,* 5918–5927.
136. Lewis, B., & von Elbe, G. (1943). Stability and structure of burner flames. *The Journal of Chemical Physics, 11,* 75–97.
137. Kim, C.-H., Jeung, I.-S., Choi, B., Kouchi, T., & Masuya, G. (2012). Flowfield characteristics of a hypermixer interacting with transverse injection in supersonic flow. *AIAA Journal, 50,* 1742–1753.
138. Micka, D. J. (2010). *Combustion stabilization, structure, and spreading in a laboratory dual-mode scramjet combustor*. The University of Michigan.
139. Mitani, T., & Kouchi, T. (2005). Flame structures and combustion efficiency computed for a Mach 6 scramjet engine. *Combustion and Flame, 142,* 187–196.
140. Sean, O. B., Ingo, S., Andrew, N., Russell, B., Neil, M., & Frank, H. (2005). OH PLIF imaging of supersonic combustion using cavity injection. In *AIAA/CIRA 13th International Space Planes and Hypersonics Systems and Technologies Conference* (p. 3357). AIAA.
141. Tarun, M., Mark, G., Kevin, J., Jeff, D., & Wayne, D. (2001). Supersonic combustion experiments with a cavity-based fuel injector. *Journal of Propulsion and Power, 17,* 1305–1312.
142. Vinogradov, V. A., Shikhman, Y. M., & Segal, C. (2007). A review of fuel pre-injection in supersonic, chemically reacting flows. *Applied Mechanics Reviews, 60,* 139–148.
143. Laurence, S. J., Karl, S., Schramm, J. M., & Hannemann, K. (2013). Transient fluid-combustion phenomena in a model scramjet. *Journal of Fluid Mechanics, 722,* 85–120.
144. Larsson, J., Laurence, S., Bermejo-Moreno, I., Bodart, J., Karl, S., & Vicquelin, R. (2015). Incipient thermal choking and stable shock-train formation in the heat-release region of a scramjet combustor. Part II: Large eddy simulations. *Combustion and Flame, 162,* 907–920.
145. Karl, S., Laurence, S., Martinez Schramm, J., & Hannemann, K. (2012). CFD analysis of unsteady combustion phenomena in the HyShot-ii scramjet configuration. In *18th AIAA/3AF International Space Planes and Hypersonic Systems and Technologies Conference* (p. 5912). AIAA.
146. Laurence, S., Ozawa, H., Lieber, D., Martinez Schramm, J., & Hannemann, K. (2012). Investigation of unsteady/quasi-steady scramjet behavior using high-speed visualization techniques. In *18th AIAA/3AF International Space Planes and Hypersonic Systems and Technologies Conference* (p. 5913). AIAA.

147. Sunami, T., Itoh, K., Satoh, K., & Komuro, T. (2006). Mach 8 ground tests of the hypermixer scramjet for HyShort-Iv flight experiment. In *14th AIAA/AHI Space Planes and Hypersonic Systems and Technologies Conference* (p. 8062). AIAA.
148. Sunami, T., & Kodera, M. (2012). Numerical investigation of a detonation wave system in a scramjet combustor. In *18th AIAA/3AF International Space Planes and Hypersonic Systems and Technologies Conference* (p. 5861). AIAA.
149. Zhu, S.-H., & Xu, X. (2017). Experimental study on flame transition in a two-stage struts dual-mode scramjet. *Journal of Aerospace Engineering, 30,* 06017002.
150. Yang, V., Li, J., Choi, J. Y., & Lin, K.-C. (2010). Ignition transient in an ethylene fueled scramjet engine with air throttling part I: non-reacting flow development and mixing. In *48th AIAA Aerospace Sciences Meeting Including the New Horizons Forum and Aerospace Exposition* (p. 409). AIAA.
151. Gruber, A., Chen, J. H., Valiev, D., & Law, C. K. (2012). Direct numerical simulation of premixed flame boundary layer flashback in turbulent channel flow. *Journal of Fluid Mechanics, 709,* 516–542.
152. Rossiter, J. E. (1964). *Wind tunnel experiments on the flow over rectangular cavities at subsonic and transonic speeds*. RAE Farnborough: Ministry of Aviation; Royal Aircraft Establishment.
153. Tim, L., Santosh, S., Sachin, K., & Clifford, S. (2007). Dynamics of bluff body flames near blowoff. In *45th AIAA Aerospace Sciences Meeting and Exhibit* (p. 169). AIAA.
154. Allison, P., Frederickson, K., Lempert, W., Sutton, J., Kirik, J., Rockwell, R., & Goyne, C. (2016). Investigation of flame structure and combustion dynamics using CH_2O PLIF and high-speed CH chemiluminescence in a premixed dual-mode scramjet combustor. In *54th AIAA Aerospace Sciences Meeting* (p. 0441). AIAA.
155. Hammack, S. D., Lee, T., Hsu, K.-Y., & Carter, C. D. (2013). High-repetition-rate OH planar laser-induced fluorescence of a cavity flameholder. *Journal of Propulsion and Power, 29,* 1248–1251.
156. Gruber, M. R., Donbar, J. M., Carter, C. D., & Hsu, K. Y. (2004). Mixing and combustion studies using cavity-based flameholders in a supersonic flow. *Journal of Propulsion and Power, 20,* 769–778.
157. Zhang, T., Wang, J., Qi, L., Fan, X., & Zhang, P. (2014). Blowout limits of cavity-stabilized flame of supercritical kerosene in supersonic combustors. *Journal of Propulsion and Power, 30,* 1161–1166.
158. Ozawa, R. I. (1971). *Survey of basic data on flame stabilization and propagation for high speed combustion systems*. OH: U. S. Air Force.
159. Barnes, F. W., & Segal, C. (2015). Cavity-based flameholding for chemically-reacting supersonic flows. *Progress in Aerospace Sciences, 76,* 24–41.
160. Namazian, M., Kelly, J. T., & Schefer, R. W. (1988). Near field instantaneous flame and fuel concentration structures. *Proceedings of the Combustion Institute, 22,* 627–634.
161. Schefer, R. W., Namazian, M., & Kelly, J. T. (1990). CH, OH, and CH_4 concentration measurements in a lifted turbulent jet flame. *Proceedings of the Combustion Institute, 23,* 669–676.
162. Donbar, J. M., Driscoll, J. F., & Carter, C. D. (2000). Reaction zone structure in turbulent nonpremixed jet flames—From CH-OH PLIF images. *Combustion and Flame, 122,* 1–19.
163. Driscoll, J. F., & Rasmussen, C. C. (2005). Correlation and analysis of blowout limits of flames in high-speed airflows. *Journal of Propulsion and Power, 21,* 1035–1044.
164. Donohue, J. M. (2014). Dual-mode scramjet flameholding operability measurements. *Journal of Propulsion and Power, 30,* 592–603.
165. Ghislain, R., Suresh, M. (2010). Experimental studies on flame stability of a fueled cavity in a supersonic crossflow. In *46th AIAA/ASME/SAE/ASEE Joint Propulsion Conference & Exhibit* (p. 6718). AIAA.
166. Le, J., Yang, S. & Li, H. (2012). Analysis and correlation of flame stability limits in supersonic flow with cavity flameholder. In *18th AIAA/3AF International Space Planes and Hypersonic Systems and Technologies Conference* (p. 5948). AIAA.

167. Rasmussen, C. C., Dhanuka, S. K., & Driscoll, J. F. (2007). Visualization of flameholding mechanisms in a supersonic combustor using PLIF. *Proceedings of the Combustion Institute, 31,* 2505–2512.
168. Rasmussen, C. C., Driscoll, J. F., Carter, C. D., & Hsu, K.-Y. (2005). Characteristics of cavity-stabilized flames in a supersonic flow. *Journal of Propulsion and Power, 21*(4), 765–769.
169. Rasmussen, C., & Driscoll, J. (2008). Blowout limits of flames in high-speed airflows: Critical damkohler number. In *44th AIAA/ASME/SAE/ASEE Joint Propulsion Conference & Exhibit* (p. 4571). AIAA.
170. Lin, K.-C., Tam, C.-J., Boxx, I., Carter, C., Jackson, K., & Lindsey, M. (2007). Flame characteristics and fuel entrainment inside a cavity flame holder of a scramjet combustor. In *43rd AIAA/ASME/SAE/ASEE Joint Propulsion Conference & Exhibit* (p. 5381).
171. Lin, K.-C., Tam, C.-J., & Jackson, K. (2009). Study on the operability of cavity flameholders inside a scramjet combustor. In *45th AIAA/ASME/SAE/ASEE Joint Propulsion Conference & Exhibit* (p. 5028). AIAA.
172. Choi, J., Ghodke, C., & Menon, S. (2010). Large-eddy simulation of cavity flame-holding in a Mach 2.5 cross flow. In *48th AIAA Aerospace Sciences Meeting Including the New Horizons Forum and Aerospace Exposition* (p. 414). AIAA.
173. Ghodke, C., Retaureau, G., Choi, J., & Menon, S. (2011). Numerical and experimental studies of flame stability in a cavity stabilized hydrocarbon-fueled scramjet. In *17th AIAA International Space Planes and Hypersonic Systems and Technologies Conference* (p. 2365). AIAA.
174. Tuttle, S. G., Carter, C. D., & Hsu, K.-Y. (2014). Particle image velocimetry in a nonreacting and reacting high-speed cavity. *Journal of Propulsion and Power, 30,* 576–591.
175. Allen, W., King, P., Gruber, M., Carter, C., & Hsu, K.-Y. (2005). Fuel-air injection effects on combustion in cavity-based flameholders in a supersonic flow. In *41st AIAA/ASME/SAE/ASEE Joint Propulsion Conference & Exhibit* (p. 4105). AIAA.